Radionuclides as Tracers of Arctic Outflows: Pathways, Water Mass Mixing, and Freshwater input to Davis Strait and the Labrador Sea

Lisa G.T. Leist[1], Maxi Castrillejo[2], Kumiko Azetsu-Scott[3], Craig Lee[4], Jed Lenetsky[5], Marc Ringuette[3], Christof Vockenhuber[1,6], Habacuc Pérez-Tribouillier[1,6], Catherine Jeandel[7], Jean-Éric Tremblay[8], and Núria Casacuberta[1,6]

[1]Institute of Biogeochemistry and Pollutant Dynamics, Department of Environmental Systems Science, ETH Zurich, Zurich, Switzerland
[2]Institute of Earth Sciences, University of Lausanne, Lausanne, Switzerland
[3]Bedford Institute of Oceanography, Dartmouth, Nova Scotia, Canada
[4]Applied Physics Laboratory, University of Washington, Seattle, Washington
[5]Department of Atmospheric and Oceanic Sciences and Institute of Arctic and Alpine Research, University of Colorado - Boulder, Boulder, Colorado, USA
[6]Laboratory of Ion Beam Physics, Department of Physics, ETH Zurich, Zurich, Switzerland
[7]LEGOS, Université de Toulouse, CNRS, IRD, CNES, UPS, Toulouse, France
[8]Département de biologie, Québec Océan and Takuvik Joint International Laboratory (UMI 3376), Université Laval (Canada)-CNRS (France), Université Laval, Québec, Canada

Correspondence: Lisa Leist (lisa.leist@usys.ethz.ch) and Núria Casacuberta (cnuria@ethz.ch)

Abstract. ~~The Davis Straitis~~ In Davis Strait, one of two ~~key Arctic gateways , where waters derived from the Atlantic flow northward and exchange with Arctic-origin waters flowing southward. This interaction may play a crucial role in shaping the formation of deep water masses~~ primary Arctic gateways between the Arctic and Atlantic Oceans, the exchange between northward-flowing Atlantic waters and southward-flowing Arctic waters possibly influences deep-water formation in the subpolar North Atlantic. Yet, these circulation pathways and mixing processes, that may be changing, remain uncertain, underscoring the need for new tracers to resolve their structure and variability. This study employs observations from 2022 and 2024 of ~~the~~ two artificial radionuclides, ^{129}I and ^{236}U ~~measured~~ as new tracers of water masses in Baffin Bay, Davis Strait and the Labrador Sea. Samples were collected during three expeditions: the AZOMP occupation of the AR7W Line in May 2022, ~~the~~ Davis Strait Observation ~~Programme~~ Program in October 2022, and the Amundsen Expedition as part of the Refuge Arctic and Transforming Climate Action programme in September-October 2024. By defining the characteristic ^{129}I and ^{236}U concentrations of the main inflowing ~~water masses (endmembers)~~waters, we examined the distribution, origin and formation of key ~~Baffin Bay water masses . This approach also allowed us to quantify the contribution of Transition Water to the formation of Labrador Sea Water (LSW) and North East Atlantic Deep Water (NEADW).~~ water masses in Baffin Bay. Our results reveal a substantial contribution (75%) of West Greenland Shelf Water to Arctic Water on the surface of central Baffin Bay~~, accounting for approximately 30%. High~~ . ^{236}U ~~identified a previously unknown pathway of~~ -rich Arctic-Atlantic-derived ~~waters~~ water entering Baffin Bay via Lancaster Sound ~~, contributing 40-50~~contributes 40 – 60% to the formation of ~~Transition Water~~the Transition Water observed in Baffin Bay. In contrast, cold Arctic Water appears to originate mainly from Nares Strait, ~~with contributions of~~ and is derived primarily (up to 70%) from Arctic-Atlantic ~~Water outflowing Nares Strait reaching up to~~

35% Water. Notably, the contribution of fresh the Baffin Bay Transition Water to the formation of LSW was significant, exceeding 3020%. However, the binary mixing model showed limitations in quantifying the origin of NEADW North East Atlantic Deep Water due to low tracer concentrations and the likely influence of multiple water mass sources. This study offers novel insights into the origin and transformation of waters water in Baffin Bay and the Labrador Sea and enhances our understanding of the complex interactions between the Arctic Ocean and the subpolar North Atlantic.

1 Introduction

1.1 The Davis Strait, connecting the Arctic with the subpolar North Atlantic

Davis Strait, located between west situated between western Greenland and Baffin Island (Fig. 11A), plays a crucial role in is a key gateway for the exchange of water masses between the Arctic Ocean and the North Atlantic oceans (Haine et al., 2015; Curry et al., 2014; Huang et al., 2024; Rudels et al., 2004; Komuro and Hasumi, 2005). The 1060 m deep sill of Davis Straitmarks , with a depth of approximately 1060 m, defines the southern boundary of Baffin Bay (max. depth of maximum depth 2300m m) and the northern boundary of the Labrador Sea (maximum depth 3500 m), which receives approximately 2 Sv (1 Sv = 10^6 m^3s^{-1})of . Through this passage, cold and fresh southward-flowing Arctic waters through multiple channels: from the central Arctic through Nares Strait , and from waters formed in Baffin Bay meet the northward-flowing warm Atlantic waters entering from the Labrador Sea. Both the fluxes and the water mass properties in Davis Strait exhibit pronounced seasonal variability (Cuny et al., 2005; Curry et al., 2014). The largest changes in temperature and salinity originate from modifications within Baffin Bay, which receives Arctic-derived waters via the main channels of the Canada Basin through the Canadian Arctic Archipelago (CAA)(Münchow et al., 2015; Rudels, 2011; Tang et al., 2004; Pelle et al., 2024). Davis Straitalso receives about 3 Sv of northward-flowing Atlantic water . These include Nares Strait, connecting to the Eurasian Basin, as well as Lancaster Sound and Jones Sound, which link to the Canada Basin (Münchow et al., 2015; Rudels, 2011; Tang et al., 2004; Pelle et al., 2 . While Atlantic inflow originates from the Labrador Sea. The Labrador Sea is an integral component itself forms an integral part of the subpolar gyre and a key deep convection area for represents a key site of deep convection that contributes to the Atlantic Meridional Overturning Circulation (Tang et al., 2004; Le Bras, 2023; Lozier, 2023). (AMOC), the ventilation of deep waters, and the oceanic uptake of anthropogenic CO_2 (Tang et al., 2004; Le Bras, 2023; Lozier, 2023; Rhein et al., 2017).

These evolving pathways Baffin Bay ocean exchanges and their associated variability and impacts underscore the importance of understanding the complex circulation system of the region. The general circulation , indicated in in Baffin Bay (Fig. 1A, 1A) is largely influenced by boundary currents. East of From eastern Davis Strait, the northward flowing northward-flowing West Greenland Current system (WGC, dark red arrows, Fig. 11A) transports two components along the Greenland shelf. The fresh West Greenland Shelf Water (WGSW) along the Greenland Shelf into Baffin Bay (Cuny et al., 2005; Curry et al., 2014; Huang et al., 2024) .The WGC , dark red), transported by the West Greenland Coastal Current, and the warm and saline West Greenland Irminger Water (WGIW, light green arrow Fig. 1A), which is confined within a shelf-break jet (Lin et al., 2018; Curry et al., 2014; Huang et al., 2024 . The WGSW originates from the East Greenland Current (EGC, dark red arrowsarrow east of Greenland, Fig. 11A), which outflows Fram Strait southward and flows south along the Greenland coastshelfbreak, carrying fresh and relatively warm Polar

Surface Water (PSW) from the Arctic Ocean (Sutherland et al., 2009). After rounding the southern tip of Greenland at Cape Farewell, the EGC ~~becomes the WGC as it enters the Labrador Sea (Gou et al., 2022)~~is joined by WGIW at depth. The warm and saline WGIW originates from the North Atlantic Current (NAC, black arrows Fig. 1A), carrying water from the subtropics (Cuny et al., 2002). Towards the northern Labrador Sea, the current system of west Greenland becomes baroclinically and barotropically unstable due to the steep continental slope, leading to large anticyclonic eddies. The eddies are known as Irminger Rings and carry both the WGSW and WGIW offshore into the Labrador Sea (Chanut et al., 2008; Zou et al., 2024; Gelderloos et a . In the northern Labrador Sea~~it~~, the WGC bifurcates into two branches, with one continuing north into Baffin Bay, and ~~another (larger)~~ a larger branch following the bathymetry of the Labrador Sea, turning ~~westwards~~ westward towards the Labrador Shelf ~~(Myers et al., 2009). In the Labrador Sea, the WGC is joined by a branch of the North Atlantic Current (NAC, black arrow Fig. 1A), which transports saline West Greenland Irminger Water (WGIW, light green arrow Fig. 1A) originating from the subtropics (Cuny et al., 2002).~~ (Myers et al., 2009; Huang et al., 2024; Gou et al., 2022).

Western Davis Strait is dominated by the southward-flowing surface Baffin Island Current (BIC, orange arrow Fig. ~~1~~1A), which transports fresh water of Arctic origin, such as Arctic Water (AW) and cold Arctic Water (cold AW), along the Baffin Island ~~margin~~ shelf and slope to the Labrador Sea (Cuny et al., 2005). ~~The~~ While Arctic Water is ~~considered of Arctic origin with a strong influence of glacial runoff, air-sea fluxes,~~ strongly influenced by glacial run-off and sea ice melt ~~(Curry et al., 2014), while the~~ (Curry et al., 2014; Azetsu-Scott et al., 2012), cold Arctic Water (similar to the hydrographic properties of cold Polar Water~~(Huang et al., 2024)~~; Huang et al. (2024)) represents a subset of cold and more saline water within ~~the~~ Arctic Water, which ~~may receive less freshwater and experience~~ experienced winter convection by stronger cooling and salinification ~~. After entering~~ (Shan et al., 2024). Waters exiting the Arctic Ocean enter Baffin Bay through the shallow sills of Nares Strait ~~(220 m, Jackson et al. (2014); Rabe et al. (2010)), Lancaster Sound (125 m, Peterson et al. (2012))~~ (220 m, Jackson et al., 2014; Rabe et al., 2010), Lancaster Sound (125 m, Peterson et al., 2012) and Jones Sound ~~(125 m, Melling et al. (2008)), these~~ (125 m, Melling et al., 2008; Pelle et al., 2024). These water masses with low salinities (<33.5) and low temperatures (<1°C) are present primarily at the surface of Baffin Bay and along the BIC.

In central Davis Strait, at intermediate depths between 300 m and 600 m, relatively warm Transition Water (dark blue Fig. ~~1~~1A) flows throughout the year and at low velocities ~~off~~ out of Baffin Bay (Huang et al., 2024; Curry et al., 2014). Rudels (2011) described Transition Water as an intermediate layer formed by mixing Atlantic water from the south and colder ~~waters~~ water from the north. More recently, Huang et al. (2024) identified two different types of Transition Water, each resulting from the mixing of several water masses. Further, Lehmann et al. (2022) identified a temperature maximum in western Baffin Bay aligning with the warmest and deepest fraction of Transition Water. Below Transition Water, down to 1600 m depth, the water column is dominated by Baffin Bay Mode Water (BBMW), also known as Baffin Bay Deep Water, whose formation processes remain unclear ~~(Huang et al., 2024; Bourke et al., 1989)~~(Lehmann et al., 2019; Bourke et al., 1989). In central Baffin Bay, depths greater than 1600 m are filled by ~~the~~ old Baffin Bay Bottom Water (BBBW) (Bourke et al., 1989), which ~~does not outflow Davis Strait~~ is not observed in the Davis Strait outflow (Curry et al., 2014).

~~Inflowing into the Labrador Sea~~South of Davis Strait, the cold, fresh surface ~~waters~~ water from the BIC ~~join~~ joins the Labrador Current, where they mix with ~~waters~~ water from the WGC that turned westward, bathymetrically steared at the Labrador Sea

(García-Ibáñez et al., 2015; Cuny et al., 2002; Myers, 2005).

In the Labrador Sea, ~~waters transported by the WGC may entrain eddies that~~ the Irminger Rings detach from the boundary current and drift into the central basin. ~~These waters also contribute~~ This water contributes to the formation of Labrador Sea Water (LSW, ~~orange arrow~~ light blue arrows in Fig. ~~1~~1A), together with fresh ~~waters~~ water from the Labrador Current, which ~~account~~ accounts for approximately 6-8% of LSW (Myers, 2005; Lilly et al., 2003; Hátún et al., 2007). The annual deep winter convection that forms the LSW represents a key component of the ~~Atlantic Meridional Ocean Circulation~~ AMOC (Yashayaev, 2007; Bower et al., 2009; Lavender et al., 2005). Other water masses in the Labrador Sea include the North East Atlantic Deep Water (NEADW, yellow arrow in Fig. 1A), which follows the cyclonic Deep Western Boundary Current and is found below LSW at approximately 2000 m depth. The NEADW forms by mixing of multiple source ~~waters inflowing~~ water inflows from east of Greenland, including LSW, Denmark Strait Overflow Water (DSOW, dark green in Fig. ~~1~~1A), and Iceland Scotland Overflow Water (ISOW, light green in Fig. ~~1~~1A) (Yashayaev, 2007; Tanhua, 2005; Dickson and Brown, 1994; García-Ibáñez et al., 2015). The bottom depths are occupied by DSOW and carried primarily by the Deep Western Boundary Current from its formation region in the Nordic Seas towards the Grand Banks (Dale et al., 2024; Leist et al., 2024; Rudels, 2011).

Decades of oceanographic studies have significantly improved our understanding of water mass composition and volumetric transport in Davis Strait, Baffin Bay, and the Labrador Sea (Bourke et al., 1989; Yashayaev, 2007; Curry et al., 2011). However, climate-driven changes are altering the circulation and freshwater dynamics of the region (Shan et al., 2024). ~~The Arctic Ocean~~ Under climate change, the Arctic is warming at nearly four times the global average~~under climate change~~, yet current ocean models appear to under-represent this rapid evolution (Rantanen et al., 2022). Observational evidence shows that weakened stratification in the Arctic Ocean is driving structural changes in the water column—a process known as ~~atlantification~~"Atlantification". This shift enables warm Atlantic ~~waters~~ water to penetrate further north, accelerating sea ice melt and reducing winter sea ice formation (Polyakov et al., 2025, 2017; Wang et al., 2024). Historically, approximately half of the exported Arctic freshwater has been exported through the ~~Canadian Arctic Archipelago (CAA)~~ CAA and into Baffin Bay (Haine et al., 2015). In recent years, increased glacial melt from Greenland and the CAA ~~(Rudels, 2011; The IMBIE Team, 2020; Gardner et al., 2011)~~ (The IMBIE Team, 2020; Vandecrux et al., 2024; Gardner et al., 2011) has led to more frequent ice-free channels during summer (Canadian Ice Service; http://ice-glaces.ec.gc.ca/), likely modifying freshwater exchange between the Arctic and Baffin Bay (Malles et al., 2025). Furthermore, Baffin Bay now receives increasing volumes of ~~Greenland glacier meltwater~~ glacier meltwater from Greenland, a trend accelerated by the warming influence of Atlantic ~~waters~~ water (Holland et al., 2008; Bamber et al., 2018).

~~Established~~ The established pathways of water mass exchange between high latitudes and the subpolar North Atlantic may also be changing ~~(Weijer et al., 2022; Carmack et al., 2016)~~(?Carmack et al., 2016). Freshwater discharge (water with practical salinity below 34.6~~PSU~~ , Zhang et al. (2021a)) from ~~the~~ Davis Strait into the subpolar North Atlantic is projected to increase, potentially affecting deep convection in the Labrador Sea (Zhang et al., 2021b; Wang et al., 2023; Yashayaev, 2024; Zhang et al., 2021a). Despite Davis Strait's ~~critical~~ role as a ~~changing~~ freshwater source to the subpolar North Atlantic ~~(Shan et al., 2024)~~ (Shan et al., 2024; Azetsu-Scott et al., 2012; Huang et al., 2024), the freshwater dynamics of both Davis Strait and Baffin Bay

remain poorly constrained. This is largely due to strong seasonal variability in freshwater release and the limited access during winter imposed by sea ice cover (Curry et al., 2014; Haine et al., 2015).

~~Despite the limitations in assessing the water mass formation in Baffin Bay~~Additionally, the contribution ~~from the Labrador Sea to the Baffin Bay, via Davis Strait, is well studied. However, the contribution~~ of water outflowing Davis Strait on the water mass formation in the Labrador Sea remains uncertain. This is likely due to intense winter convection in the Labrador Sea, which strongly modifies temperature and salinity, complicating efforts to trace the origins of water using only these properties (Rudels, 2011; Yashayaev, 2007; Clarke and Gascard, 1983).

~~The~~ Furthermore, the role of Baffin Bay intermediate and deep ~~waters~~ water (e.g. Transition Water) in the formation of LSW remains poorly understood compared to the better-known origin and pathways of surface ~~waters (Curry et al., 2014; Cuny et al., 2005) . Recent~~ water (Curry et al., 2014; Cuny et al., 2005). Also, recent studies have emphasised the importance of Arctic freshwater export to the subpolar North Atlantic (Malles et al., 2025; Duyck et al., 2025; Myers, 2005) and the role of cross-density lateral mixing in the Labrador Sea, contributing approximately 60% to the annual formation of LSW (Zou et al., 2023; Pickart and Spall, 2007). However, most observational studies continue to focus on boundary current systems, leaving off-boundary water exchanges understudied (Huang et al., 2024; Curry et al., 2011; Azetsu-Scott et al., 2012)~~, which could be crucial to understanding phytoplankton bloom formation and carbon cycling/sequestration (Boyd et al., 2019)~~. Therefore, a better understanding of the off-shelf and intermediate circulation between Baffin Bay and the Labrador Sea is still needed (Rudels et al., 2004), particularly regarding the origin and formation of Transition Water ~~and~~ in Baffin Bay and the potential contributions of Arctic origin freshwater to the formation of LSW.

1.2 Using radionuclides to trace water mass origin

To advance on these complex water-mass interactions, we propose a novel approach in the region that combines the two long-lived artificial radionuclides ^{129}I (~~T~~$t_{1/2}$=15.7 Ma) and ^{236}U (~~T~~$t_{1/2}$=23.4 Ma), with ~~conservative hydrographic properties (~~hydrographic properties such as salinity and temperature~~)~~. We expect ^{129}I and ^{236}U to suitably trace circulation patterns and mixing in the Davis Strait region because inflowing ~~waters present~~ water presents contrasting tracer concentrations measured ~~upstream in~~ for the Pacific, Atlantic and Arctic oceans ~~(Wefing et al., 2021; Payne et al., 2024; Leist et al., 2024)~~ (Wefing et al., 2021; Payne et al., 2024; Leist et al., 2024; Castrillejo et al., 2018; Dale et al., 2024).

^{129}I and ^{236}U originate primarily from nuclear sources and are assumed to be conservative in seawater (Christl et al., 2015; Casacuberta and Smith, 2023). Their input into the ocean was dominated by a peak in ^{236}U from the ~~global fallout from nuclear weapons testing~~ nuclear weapons test global fallout in the 1960s, and liquid releases from nuclear fuel reprocessing plants in Sellafield (UK) and La Hague (France) (Fig. 1A, black factory symbols), peaking in the 1980s for ^{236}U and ramping up after 1990s for ^{129}I. Fig. ~~A1~~ A1 represents their input function defined at 70°N (blue star in Fig. 1A), a combination of global fallout and liquid releases from the nuclear reprocessing plants (Wefing et al., 2021; Payne et al., 2024). In both cases, the released radionuclides flow north from the North Sea and join the Norwegian Coastal Current (NCC), entering the Arctic Ocean. From the entrance of the Arctic Ocean, the radionuclides can recirculate within the ~~Arctic~~ Eurasian Basin in a short loop ~~(central Arctic)~~ or a longer path (Canada Basin) before exiting the Arctic Ocean via Fram Strait or the CAA (Li et al., 2020; Rudels

et al., 1994; Payne et al., 2024; Casacuberta and Smith, 2023). From Fram Strait, the radionuclides are transported south and ultimately reach the Labrador Sea and Baffin Bay as part of the WGC (Wefing et al., 2019; Dale et al., 2024; Leist et al., 2024). Up to date, there are no measurements of these two tracers in either Nares Strait or the CAA, so their transport through these routes is still unknown.

In the Arctic Ocean, the transport times and mixing of Atlantic Water can be calculated using ~~the input function shown in~~ different models that are all based on tracer input functions (Fig. ~~A1~~ A1) (Wefing et al., 2021; Payne et al., 2024). However, in sub-Arctic regions, the simultaneous mixing of multiple water masses with distinct input functions complicates the accurate estimation of water age and mixing when relying solely on these tracers. Nevertheless, the combination of ^{129}I and ^{236}U has already ~~proved~~ proven to be a suitable ~~tracer of~~ tool to study the formation and origin of ~~the water mass~~ water masses in the subpolar North Atlantic, where it can be assumed that both tracers are in a steady state for each water mass (Castrillejo et al., 2018; Leist et al., 2024; Dale et al., 2024). ~~This is a valid assumption, since recent changes (approximately 20 years) in the input function are small compared to changes caused by the mixing of different water masses, each carrying a distinct tracer signal.~~

In the study area, we expected to find a wide representation of the historical temporal variation of the tracers, allowing us to disentangle the origin of Atlantic ~~waters:~~ water. While the "old" Arctic-Atlantic ~~water~~ Water (AAW) from the Canada Basin would be characterised by high ^{236}U and low ^{129}I (Payne et al., 2024), the "young" ~~Arctic-Atlantic water~~ Polar Surface Water (PSW) recirculated in the ~~central Arctic~~ Eurasian Basin would carry a higher signal of ^{129}I (Wefing et al., 2025). Low tracer concentrations should be characteristic of the WGIW, which enters the study region from the subtropics without direct contact with ~~reprocessing~~ the radionuclides (Castrillejo et al., 2018; Dale et al., 2024; Leist et al., 2024). Also, Pacific Water (salinity of 32.5~~PSU~~) entering Baffin Bay through CAA would carry low concentrations of both radionuclides, as their only source was the atmospheric weapon tests (Payne et al., 2024). Finally, it is important to note that the freshest ~~waters~~ water (i.e. glacier melt, sea ice melt, and river ~~runoff~~run-off; Shadwick et al. (2011); Grenier et al. (2022); Bamber et al. (2018); Malles et al. (2025)) should contain almost no tracer, hereinafter denoted as tracer-free ~~waters~~water (Casacuberta et al., 2016).

In this study, we address critical knowledge gaps in ~~the understanding of~~ understanding water mass transformations and exchanges between Baffin Bay, Davis Strait and the Labrador Sea by applying a novel approach based on the two long-lived artificial radionuclides, ^{129}I and ^{236}U. The tracers, which exhibit distinct distributions across Arctic and Atlantic origin water, offer a complementary tool to traditional hydrographic parameters such as temperature and salinity, enabling the identification of water mass sources in regions characterised by complex mixing and strong seasonal variability. Using observations collected between 2022 and 2024 across key Arctic gateways —including Davis Strait, Nares Strait, Lancaster Sound— and the Labrador Sea, we apply a binary mixing model to characterise tracer signatures of inflowing water masses and quantify their contributions to key intermediate and deep water masses. This approach allows us to explore the origin of the Transition Water, ~~Baffin Bay Mode Water and~~ BBMW, BBBW and (cold) Arctic Water and to follow the evolution of ~~West Greenland Shelf Water and West Greenland Irminger Water. It further allows for the evaluation of the~~ WGSW and WGIW along their cyclonic journey through

the Baffin Bay. It also enables us to assess the potential influence of Transition Water on water mass formation ~~processes~~ in the Labrador Sea.

2 Methods

2.1 Sample collection and processing

Seawater samples were collected from multiple sites (Fig. 1B). In May 2022, along the AR7W Line across the Labrador Sea, seawater was collected from the surface and six depth profiles ~~along~~ (depth range: surface - 3560 m), including four surface samples from southwest of the AR7W Line~~across the Labrador Sea~~ , aboard R/V Atlantis as a part of the Atlantic Zone Off-Shelf Monitoring Program (AZOMP) by Bedford Institute of Oceanography (red triangles). In October 2022, additional sampling was conducted in the Davis Strait region aboard R/V Neil Armstrong as part of ~~the~~ Davis Strait Observing System ~~(DSOS)~~ Program. This survey included a depth profile in central Baffin Bay (Fig.~~1~~ 1B, red square, depth range: surface - 2377 m), and full transects along the Northern Line (9 stations, Fig. ~~1 red circles~~1B red circles, depth range: surface - 1665 m), Davis Strait ~~Mooring Line~~ (10 stations, red diamonds Fig. ~~1B~~1B, depth range: surface - 1013 m) and Northern Labrador Sea Line (9 stations, Fig. ~~1 red stars~~1B red stars, depth range: surface - 2614 m). Further sampling was conducted in September-October 2024 during the ~~Transforming Climate Action~~ Refuge Arctic Cruise Legs 4 and Transforming Climate Action Leg 5, both onboard CCGS Amundsen, targeting Nares Strait and Lancaster Sound. In northern Nares Strait~~(Fig. 1B) unfilled orange square), ~~ , two stations were sampled: one depth profile (50-345 m, ~~St. NS89) was sampled along with a single-depth station (NS79). In the southern Nares Strait~~ (RA28) and one surface station (RA34). Both are represented in Fig. ~~1B) unfilled orange circle), located south of the sill, four~~ 1B as one unfilled orange square. In the southern Nares Strait, three stations were sampled~~, NS102 to NS114, with one~~ : RA44, RA48, RA50, of which only RA48 is a depth profile (70-600 m)~~at NS107.~~ . These stations are represented in Fig. 1B as unfilled orange circles. In Lancaster Sound, two sites were sampled in the western part ~~within~~ of the Archipelago (Keb/TCA-S3, depth range: 2-140 m, unfilled red triangles in Fig. ~~1B)unfilled red triangle, KEBABB S3~~1B), ~~2-140 m),~~ and the eastern part ~~neighbouring~~ close to Baffin Bay (~~Fig. 1B) unfilled red diamond,~~ TCA S3, depth range: 2-890 m, unfilled red diamond in Fig. 1B). All cruises ~~included~~ used a CTD-Rosette equipped with 24-12 L Niskin bottles ~~, which were used to collect seawater~~to collect samples for the purpose of this study.

~~The seawater~~ Seawater samples for ^{129}I analysis were collected in 250 ml ~~opaque~~ brown plastic bottles, and pre-rinsed three times with ~~the sample before filling~~water from the Niskin bottle, before being filled. For ^{236}U, 2-3 L of seawater were collected in Nalgene ~~Cubitainers~~cubitainers, also pre-rinsed three times before filling them. All samples were stored ~~unprocessed and~~ onboard without any further processing, sent to ETH Zurich for the analysis of iodine and uranium isotopes.

The radiochemistry of ^{129}I and ^{236}U was performed following Wefing et al. (2019) and Leist et al. (2024) for a total of 307 samples. The samples were analysed using the TANDY AMS ~~facility~~ system at the Laboratory of Ion Beam Physics (LIP), ETH Zurich (Vockenhuber et al., 2015). ~~Reproducibility~~ The ^{129}I concentrations were calculated using the measured ^{127}I/^{129}I atom ratio and the known amount of spiked ^{127}I. The reproducibility of ^{129}I data was estimated based on repeated measurements of an internal seawater standard (n=14, average ^{129}I= 10.4~~±~~±0.5×10^{7} at/kg). Blanks for ^{129}I (n=16, ~~1.2~~7.6±1.5~~×10^{7} at/kg~~×10^{5}

at) were obtained using deionised water treated following the same procedure as for seawater samples.

The samples for ^{236}U were spiked with 1 pg of ^{233}U following the radiochemistry described by Wefing et al. (2021) and Leist et al. (2024). The MILEA AMS ~~facility at LIP~~ system at LIP facility (Christl et al., 2013, 2023) was used to measure ^{233}U/^{238}U and ^{236}U/^{238}U in the samples and the in-house standard "ZUTRI". Correction procedures were applied as described by Christl et al. (2023). The concentrations of ^{236}U and ^{238}U were calculated based on the known amount of ^{233}U that was spiked in the sample. Each batch included one blank (n=11, ~~: 0.03~~^{236}U: 0.01$\pm$~~0.02$\times10^{7}$ at/kg~~0.01$\times10^{6}$ at), consisting of deionised water that was treated like the samples.

The results of ^{129}I and ^{236}U are reported and plotted in atoms per kg of seawater (at/kg). The combined uncertainty of chemical processing and measurements for both ^{129}I and ^{236}U was below 6%. ~~Detailed~~ All results and detailed analytical uncertainties are reported in the Zenodo database (https://doi.org/10.5281/zenodo.16914587).

2.2 Water mass classification

The water masses ~~(~~are summarised in Table A1~~)~~ , and were assigned according to previous ~~classifications of the water mass~~ water mass classifications in the literature ~~(Curry et al., 2014; Huang et al., 2024; García-Ibáñez et al., 2015; Bourke et al., 1989)~~ (Curry et al., 2014; Huang et al., 2024; García-Ibáñez et al., 2015; Bourke et al., 1989; Lehmann et al., 2022) and identified using conservative temperature (CT) and absolute salinity (S_A, see ~~the~~ T-S diagram in Fig. ~~A2~~A2). The conversion from practical to absolute salinity and from potential to conservative temperature was performed according to TEOS-10 (IOC and IAPSO, 2010). Temperature and salinity are also represented along sections in Fig. A3 to facilitate the comprehensive distribution of water masses. West Greenland Irminger Water (WGIW; CT > 3.5°C, S_A > 34.7) is the warmest and most saline water mass, confined to intermediate depths along the Greenland shelf~~(Fig. A3E–H).~~ . West Greenland Shelf Water (WGSW; CT < 5°C, S_A < 34.2) is fresher than WGIW and located at the surface along the Greenland shelf~~(Fig. A3A–D).~~ . Arctic Water (AW; ~~1.1 > CT>~~ CT: -0.8 – 1.1°C, S_A > 32.9) is the freshest water mass, confined to the Baffin Island and Canadian shelf~~regions~~. The CT and S_A ranges used here differ significantly from those in Curry et al. (2014); we applied a narrower range for Arctic Water and distinguished it from cold Arctic Water (cold AW; CT ~~>~~ < -0.8°C, 32.5 < S_A < 33.8), which is colder and more saline. Below the cold Arctic Water, Transition Water (CT ~~: 1.4 –~~ < 1.8~~°C~~, S_A~~= 34.6 ± 0.2) and its fresher variant, Transition Watermix (CT<~~ : 34-34.6) is characteristic of mid-depth in Baffin Bay and Davis Strait. Within Transition Water, temperature increases with depth to a temperature maximum (CT: 1.4 – 1.8°C, S_A = ~~34.0–34.5), are characteristic of Baffin Bay and Davis Strait~~34.64 ± 0.03, Lehmann et al. (2022)). In Baffin Bay, at depths of 600 – 1000 m, Baffin Bay Mode Water (BBMW; CT: 0.7 – 1.2°C, S_A = 34.6; ~~(Huang et al., 2024)~~Huang et al. (2024)) was observed overlying Baffin Bay Bottom Water (BBBW; CT < 0.4°C, S_A = 34.6; ~~(Bourke et al., 1989)~~Bourke et al. (1989), Fig. A3). In the Labrador Sea~~(Fig. A3C, D, G, H),~~ , Labrador Sea Water (LSW; CT: 3.1 – 3.8°C, S_A ~~=~~ > 35.0; ~~(García-Ibáñez et al., 2018)~~García-Ibáñez et al. (2018)) resides at intermediate depth. Beneath LSW, North East Atlantic Deep Water (NEADW; CT~~between~~ : 2.0 ~~and~~ - 3.3°C, S_A = 35.07 ± 0.2; ~~(Yashayaev, 2007)~~Yashayaev (2007)) overlies Denmark Strait Overflow Water (DSOW; CT < 1.3°C, S_A = 35.0 ± 0.1; ~~(García-Ibáñez et al., 2018)~~García-Ibáñez et al. (2018)). In Nares Strait and Lancaster Sound, water masses were classified as Arctic Water CAA (AW_{CAA}; CT < 0°C, S_A < 33) and Arctic Atlantic Water CAA (AAW_{CAA}; CT > -1°C, S_A > 33). Samples

that do not fall within the defined water mass categories are considered mixtures of the above water types. While all samples are presented in the results section, the discussion focuses on those assigned to specific water masses.

2.3 Binary Mixing Model

~~To quantify the origin and mixing of water masses, we used~~ In the study area, several potential water masses are adjacent to those observed in Baffin Bay. These include tracer-free water, Pacific Water (Azetsu-Scott et al., 2012), WGIW (Curry et al., 2014), WGSW (Curry et al., 2014), Polar Surface Water from the Eurasian Basin (Münchow et al., 2006; Wefing et al., 2025), and Arctic-Atlantic Water originating from the Canada Basin (Lehmann et al., 2022; Payne et al., 2024). Further assessment of their formation processes will be based on the conservative tracer signatures of ^{129}I and ^{236}U. However, the number of water masses considered exceeds the number of available conservative tracers. Therefore, the complexity of the model is reduced by modelling the mixing fractions of samples between the two most dominant water mass sources (hereinafter referred as endmembers), instead of employing an Optimum Multiparameter Analysis. Before quantifying the origin and estimating the mixing fractions, the water masses are classified according to their temperature and salinity. Then, a binary mixing model ~~that combines~~ combining both ^{236}U and ^{129}I~~, as~~ is used, as previously described by Leist et al. (2024) and Dale et al. (2024). The water masses in the study area are considered ~~to be the result of the conservative mixing of different source waters, referred to as endmembers, which establish the boundary tracer concentrations~~ as conservative mixtures of different endmembers. The endmembers are source components of a mixture and set the ~~model domain. Endmembers were defined according to the characteristic temperature and salinityproperties of the individual water masses identified as source components. The specific endmembers used in this study are further discussed in Section 4.1~~boundaries of the mixing model. In this study, each endmember has a distinct and characteristic value for temperature, salinity, and ^{129}I and ^{236}U concentrations (see details on each endmember in Section 4.1).

In ~~the study regions, the number of endmembers considered—up to five—exceeds the number of available tracers, introducing limitations in resolving unique mixing solutions. To simplify this complexity, mixing is modelled between the two most dominant endmembers~~ most cases, the ^{129}I and ^{236}U concentrations of the endmember consist of an average concentration of several samples collected in this and previous studies, with an associated uncertainty that corresponds to the standard deviation of the average values (see Table A2). Considering the two endmembers as the primary water-mass sources, the resulting water mass is treated as a mixture of the two. The mixing fraction f is ~~estiamted as:~~

then estimated as:

$$f = \frac{\|a\|}{\|b\|} \frac{\|\vec{a}\|}{\|\vec{b}\|} \tag{1}$$

~~Here, a denotes~~ where $\vec{b}$ is the vector connecting the two endmembers (mixing line), and $\vec{a}$ is the vector connecting a given sample to one ~~endmember, while b~~ of the endmembers. The resulting value of f represents the ~~vector between the two endmembersthat are considered most influential in the sample's formation. For the endmember the tracer mean is calculated~~

and used in the fraction estimate. One percentage contribution of each endmember to a given watermass. This study focuses on different contributions of Atlantic-derived water, and not on the differentiation between different freshwater sources, which are more precisely addressed using nutrients and $\delta^{18}O$ (Azetsu-Scott et al., 2012). A key limitation of this model is that it assumes mixing occurs only the assumption that mixing occurs exclusively between two endmembers. If a sample lies outside this falls outside the defined mixing line, it must be orthogonally projected onto the line, unless specified otherwise, to estimate its composition. In addition, endmembers are derived from different numbers of samples (see Table A2), which might influence the error rangeits composition is estimated by projecting orthogonally onto the mixing line and neglecting potential contributions from a third endmember. The model also assumes a steady state for transient tracers, which was previously discussed and justified by Leist et al. (2024) and Dale et al. (2024). In the study region, changes in water mass formation and mixing ratios between endmembers are believed to have a greater influence on tracer concentrations than recent changes in the tracer input function (Fig. A1), supporting the steady-state assumption. The resulting mixing fractions will only be discussed in Section 4 (not in results) and summarised in Table **??**.

3 Results

This section presents individual depth profiles from Nares Strait and Lancaster Sound (Fig. 2), followed by a detailed tracer description of the distribution along the three transects at from southern Baffin Bay (Northern Line), Davis Strait(Mooring Line), Northern , to northern and southern Labrador Sea (Northern Labrador Sea and AR7W lines). The results of and ^{236}U are reported and plotted in atoms per kg of seawater (at/kg). To better reflect the general distribution patterns, each water mass is described across the lines/panels (Fig. 3) as a whole, rather than within individual sections. Details about tracer concentrations, uncertainties, and hydrographic properties are provided in the Zenodo database and supporting materials. The acronyms for the (https://doi.org/10.5281/zenodo.16914587) and the abbreviations for water masses can be found in the Appendix Table A1.

3.1 ^{129}I and ^{236}U in Nares Strait and Lancaster Sound

Depth profiles collected in Nares Strait are represented in Fig. 22A and B as orange symbols. Both tracers show low concentrations at the surface Arctic Water (AW, ^{129}I: 60-85$\times10^7$ at/kg, ^{236}U: 11-14$\times10^6$ at/kg) and a local maximum in the Arctic Atlantic Water at about 250 m (AAW, ^{129}I: 180-210$\times10^7$ at/kg, ^{236}U:23$\times10^6$ at/kg). Below that depth, ^{129}I seems to slightly decrease towards the bottom, while ^{236}U remains more constant. Furthermore, the concentrations of both isotopes appear to be higher in the northern part of Nares Strait (squares) compared to the south (circles).

The two profiles in Lancaster Sound are represented in Fig. 22A and B as red symbols. Similar to Nares Strait, the highest concentrations of ^{129}I were associated with AAW$_{\mathit{CB}}$ $_{\mathrm{CB}}$ (Canada Basin) located at 200 m in eastern Lancaster Sound (^{129}I: 130$\times10^7$ at/kg, S_A: 33.85, CT: -0.10) and at depths below 140 m in the western station (^{129}I: 120$\times10^7$ at/kg, S_A: 33.6, CT: -0.44). In western Lancaster Sound, the highest concentration of ^{236}U was observed at 10 m depth in the Arctic Water (^{236}U: 19$\times10^6$ at/kg, S_A: 30.58, CT: -0.04), and the lowest at the surface (^{236}U: 15$\times10^6$ at/kg). A similar distribution was observed

in the eastern Lancaster Sound, with the lowest concentration at the surface (^{236}U: 13×10^{6} at/kg), and a maximum at 200 m (^{236}U: 22×10^{6} at/kg), which then ~~slightly decreased~~ decreased slightly with increasing depth to ~~:~~15×10^{6} at/kg at 886 m.

3.2 ^{129}I and ^{236}U in central and southern Baffin Bay, Davis Strait and the Labrador Sea

Along all ~~lines~~transects (Fig. 3), the highest ^{129}I concentrations were observed in West Greenland Shelf Water (WGSW), at the surface of the Greenland shelf (Fig. ~~3~~3A-D). The concentrations of ^{129}I ~~concentrations~~ decreased along the pathway of the West Greenland Current (WGC), with WGSW dropping from 320 ×10^{7}at/kg at AR7W in the Labrador Sea (Fig. ~~3~~3D) to 170×10^{7} at/kg at the Northern Line in Baffin Bay (Fig. ~~3~~3A). In contrast, the warmest and most saline West Greenland Irminger Water (WGIW) generally showed increasing ^{129}I concentrations from 50×10^{7} at/kg at AR7W ~~(Fig. 3D)~~ to a maximum of 90×10^{7} at/kg at the Northern Line~~(Fig. 3A). In AW~~, In Arctic Water, the freshest water along the Baffin Island Current (BIC) and Labrador Current (LC), ^{129}I concentrations increased slightly from central Baffin Bay (140×10^{7} at/kg, blue squares Fig. ~~2~~2C) to the Northern Labrador Sea Line (150×10^{7} at/kg, Fig. ~~3C), but~~ 3C). But, Arctic Water showed lower concentrations (100×10^{7} at/kg) at the AR7W Line in the southern Labrador Sea. Cold Arctic Water exhibited elevated ^{129}I concentrations in the ~~100-170~~100 – 170×10^{7} at/kg range and showed no clear north-south trend. While ~~AW~~Arctic Water, WGIW and WGSW were present in all sections, Transition Water was only present along the ~~Mooring Line, Northern Line~~Northern Line, Davis Strait (Fig. ~~3B, A~~3A, B) and central Baffin Bay (Fig. ~~2~~2C, blue squares), with concentrations in the range of ~~50-120~~50 – 120×10^{7} at/kg, respectively. BBMW was observed along the Northern Line, Davis Strait and central Baffin Bay only, with ^{129}I concentrations ~~at~~ of 29 – 37×10^{7} at/kg. ^{129}I concentrations at the levels of the blanks (<~~1.2 ± 1.5 × 10^{7}~~ 1.2 ± 1.5×10^{7} at/kg) were measured in BBBW present below 1600 m in central Baffin Bay and the Northern Line. Labrador Sea Water (LSW) and North East Atlantic Deep Water (NEADW) (only sampled at AR7W, Fig. ~~3~~3D) covered an ^{129}I range of 30-70×10^{7} at/kg at intermediate depth in the Labrador Sea, while the near-bottom Denmark Strait Overflow Water (DSOW) presented concentrations up to 120×10^{7} at/kg.

The distribution of ^{236}U concentrations (Fig. ~~3E-H~~3E – H) differs from that of ^{129}I. The highest ^{236}U was observed in ~~waters outflowing through Davis Strait~~ the Transition Water (Fig. ~~3H~~3E, F), ~~particularly~~ with up to 19×10^{6} at/kg in central Baffin Bay (Fig. ~~2~~2D, blue squares), followed by cold ~~AW~~Arctic Water, with ^{236}U in the 14-17×10^{6} at/kg range between ~~the Mooring Line~~ Davis Strait (Fig. ~~3~~3F) and central Baffin Bay. While the ^{236}U concentration in Arctic Water was generally in the range of ~~13-15~~13 - 15×10^{6} at/kg, the AR7W Line recorded the maximum value (16×10^{6} at/kg, Fig. ~~3~~3H). In water inflowing Davis Strait, such as WGSW, ^{236}U concentrations decreased slightly towards the north, from 15×10^{6} at/kg at the AR7W Line to 13×10^{6} at/kg at the Northern Line (Fig. ~~3~~3E). Similarly to ^{129}I, low ^{236}U concentrations were measured in WGIW, with an increasing trend from 9×10^{6} at/kg at AR7W to 11×10^{6} at/kg on the Northern Line.

In the Labrador Sea, LSW presented ^{236}U concentrations on the 9-11×10^{6} at/kg range on the AR7W and Northern Labrador Sea lines (Fig. ~~3H, G~~3G, H). NEADW, only sampled along AR7W, showed ~~again~~ ^{236}U concentrations slightly above LSW (10-12×10^{6} at/kg). The sampling density of DSOW was smaller in the Northern Labrador Sea Line than for AR7W and confined at slightly lower concentrations (AR7W: 12-14×10^{6} at/kg, Northern Labrador Sea Line: 12×10^{6} at/kg). Moving towards the Baffin Bay, the BBMW had similar ^{236}U concentrations of 10-12×10^{6} at/kg. Finally, in BBBW occupying depths

below 1600 m in central Baffin Bay (blue squares Fig. ~~2~~2D) and the Northern Line, ^{236}U concentrations reached the ~~detection limit~~ analytical limit of detection ($1.2 \pm 1.5 \times 10^6$ at/kg).

Both tracers have concentrations well above ~~the global falloutlevels~~global fallout, which would be ~~of~~ about 2.2×10^7 at/kg for ^{129}I and 5.4×10^6 at/kg for ^{236}U~~–~~, according to recent estimates at the Bering Strait ~~(Payne et al. , in prep).~~ (Payne, 2026). Only the bottom water at Baffin Bay (BBBW) presents tracer concentrations lower than expected from the global fallout.

3.3 Water masses in ~~T-S~~ T – S and ^{129}I ~~-~~ – ^{236}U tracer space

Figure 4 provides an overview of the ~~distribution of the water masses in T-S space~~ water masses observed in Baffin Bay, Davis Strait and the Labrador Sea and their distribution in T – S diagram (Fig. 4A) and ^{129}I ~~-~~ – ^{236}U tracer space (Fig. 4B) ~~. In addition to the water mass description in Section 2.2, here the water masses have been further defined by looking at the radionuclide tracers. For example, in some cases, the and concentrations are used to define the same water mass that changed the properties of temperature and salinity, but the tracer concentration remained the same (for example, WGSW in~~ while the sampling location is indicated by the ~~AR7W Line falls within the temperature and salinity range of Arctic Water (~~symbols and can be referred to in Fig. ~~4A and Bindicated by black cirles), as the tracer concentration results almost exclusively from mixing between endmembers. This is important to keep in mind in an area strongly affected by seasonality (Curry et al., 2014; Shan et al., 2024) . The sampling of AR7W took place in spring, while the Northern Labrador Sea, Mooring and Northern lines, as well as the central Baffin Bay, were sampled in autumn.~~ 1B.

WGSW (~~dark red symbols) is prominent in both graphs~~ dark-red symbols) stands out in both panels due to its relatively high temperature and low salinity (Fig. ~~4~~ 4A), ~~and because it contains the highest~~ as well as its elevated ^{129}I concentrations (from 180 to >300 $\times 10^7$ at/kg) (Fig. 4B). ~~Although seasonal variability is represented in the broad temperature range~~ Its seasonal variability in temperature (Fig. 4A) ~~and is observed by , e.g.~~ is consistent with observations by Curry et al. (2014) and Zweng and Münchow (2006) ~~, the tracer space shows~~ and clearly expressed in the broad temperature range with CT$<$ 0 °C along the AR7W Line (dark red triangles) sampled in spring and CT$>$ 2 °C at the other sections sampled in autumn. In the tracer WGSW, space forms a well-defined ~~line, suggesting~~ linear relationship, despite the seasonality. This indicates that the tracers are largely insensitive to seasonal changes. ~~Transition Water (dark blue symbols) , located between cold Arctic Water~~ The saline and warm WGIW (Fig. 4A, light green symbols) is located at the lower left in tracer space (Fig. 4~~teal symbolswith golden edges) and WGIW/LSW (mint/orange symbols) in T-S space, shows the highest~~ B, light green symbols) due to its low ^{129}I and ^{236}U concentrations. Radionuclide tracers are especially low for samples collected in the Labrador Sea, then they increase slightly together with a freshening and cooling experienced on the northward flow of WGIW.

Arctic Water (Fig. 4~~B), second only to concentrations measured at Nares Strait and Lancaster Sound. Lower tracer levels in the same region correspond to fresher surface waters.Cold Arctic Water~~ , light brown symbols) is fresh and cold and shows tracer concentration slightly below cold Arctic Water (Fig. 4, teal symbols), which is characterised by its distinct temperature minimum and confined to the upper 100 m~~, is~~ . Both water masses are positioned in the tracer space at the mixing interface between the relatively warm Transition Water ~~mix and WGSW, with a clear influence from low-tracer Pacific Water or water~~

of subtropical North Atlantic origin, such as WGIWand WGSW.

The saline and warm WGIW is

Within the Transition Water (light blue symbols), the samples located at the lower left in tracer space due to its low temperature maximum (TrW_{Tmax}, dark-blue symbols) exhibit the highest ^{236}U concentrations. This TrW_{Tmax} lies between cold Arctic Water (teal symbols) and WGIW (light green symbols) in T–S space, consistent with its intermediate hydrographic character (Fig. 4A). In tracer space, however, the TrW_{Tmax} shows the highest ^{236}U levels within the region (Fig. 4B), second only to the concentrations observed in Nares Strait (orange symbols) and Lancaster Sound (red symbols).

At depth below Transition Water and low temperatures is the BBMW (light purple squares and circles) confined at low ^{129}I and intermediate ^{236}U concentration. Radionuclide tracers are especially low for samples collected in the Labrador Sea, then they increase slightly together with a freshening and cooling experienced on the northward flow of WGIW.concentrations, leading to the even deeper and colder BBBW (purple squares and circles). The BBBW in the Northern Line and central Baffin Bay is found in the lower bottom left corner of the tracer space because and its concentrations of ^{129}I and ^{236}U are extremely low and approach the analytical limit of detection. Both and increase in BBMW (light purple diamonds), with concentrations similar to the more saline and warmer LSW and NEADW in the Labrador Sea.

In the Labrador Sea, surface waters (water (light red symbols) fill the tracer concentrations fills the gap tracer between WGSW and WGIW , as well as the salinity ranges between the two water masses. Two surface samples at AR7W are well separated from the remaining surface samples. They are colder (CT around 1.5°C) and with fresher (S_A:33.8) than the other surface samples (S_A>34.2). Their tracer concentration in and bridges WGSW and LSW (blue trangles) in the T – S diagram. LSW is colder than WGIW but warmer than the deeper NEADW (yellow triangles). In the tracer space, both LSW and NEADW are located close to WGIW but shifted towards slightly higher ^{236}U (more clearly seen in Fig. 6C), is elevated relative to the other surface samples and it falls within the cluster of fresher and colder DSOW . concentrations.

Finally, DSOW (Fig. 4, green symbols), in turn, is characterised by low temperatures, high salinity, and intermediate tracer concentrations. Freshwater sources - such as sea ice and glacial meltwater, river run-off, and precipitation - are considered tracer-free; thus, their presence would be indicated by lower salinities and a spread toward low tracer concentrations.

4 Discussion

To investigate the origin and mixing of the water masses of this study, in southern Baffin Bay, Davis Strait and Labrador Sea, we apply the mixing model described in Section 2.3. HereIn this section, we first examine the endmembers used in the mixing model (Section 4.1), followed by a discussion of the evolution of West Greenland Shelf Water and West Greenland Irminger Water (WGSW and WGIW) as they enter Baffin Bay (Section 4.2). The , the origin of Transition Water, Baffin Bay Mode Water (BBMWand Baffin Bay Bottom Water (BBMW, BBBW), cold Arctic Water, and Arctic Water is then examined in (Sections 4.3 and 4.4. The discussion concludes with how all these waters contribute to the formation of Labrador Sea Water (LSW) and North East Atlantic Deep Water (NEADW,) and their evolution to the Labrador Sea (Section 4.5). An overview of the mixing fractions obtained is given in Table **??**.

4.1 Endmembers in the mixing model

~~Endmembers will be used in the binary mixing model to estimate the origin and composition of water masses. In Fig.~~ Figure 5A ~~, the geographical location~~ shows the geographical locations of the defined endmembers~~are shown as diamonds, and unfilled symbols, which are then represented in Fig. 5B with their~~ , each represented with distinct symbols and colours. Their corresponding ^{129}I and ^{236}U tracer signatures ~~, as well as the depth ranges relevant to each endmember.These endmembers (Table A2)~~ are displayed in Fig. 5B. The endmembers are defined using a combination of published data and new tracer measurements. ~~The water~~ Water mass assignments are based on ~~hydrographic properties, as explained in Section 3. For endmembers derived~~ temperature–salinity characteristics, and for endmembers taken from the literature, the original ~~classification of the water mass is maintained.~~ classifications are retained. Table A2 summarises all endmembers used in this study, including their geographic locations, depth ranges, tracer concentrations, temperature and salinity values, the number of samples included, and the relevant references.

Based on previous studies, the initial mixing scenarios (Fig. 5B) are constructed using the following endmember pairs: AAW_{CB} – Pacific Water (Peterson et al., 2012; Lehmann et al., 2022), Nares Strait outflow – Pacific Water (Melling et al., 2008) and WGSW – NAC (North Atlantic Current; Leist et al., 2024).

4.1.1 Endmembers in the subpolar North Atlantic and the Arctic Canada Basin

The NAC endmember (North Atlantic Current; turquoise diamond, Fig. 5) ~~represents the North Atlantic Current, which feeds into the WGIW . It carries water of~~ contributes to WGIW and transports mainly subtropical Atlantic ~~origin~~ water labelled with a low tracer content from global fallout and a small contribution from the European nuclear reprocessing plants (Leist et al., 2024; Castrillejo et al., 2018). Representative of this endmember ~~is a sample~~ are samples taken east of Reykjanes Ridge ~~(St. 38, SAIW, Castrillejo et al., 2018)~~(St. 38, IcSPMW, Castrillejo et al., 2018). The diluted reprocessing plant signal may originate from tracer-labelled water entering the subpolar gyre from the Labrador and Irminger seas and reaching east of the Reykjanes Ridge. The Iceland Scotland Overflow Water (ISOW), formed by deep convection north of Iceland, is represented by data collected before entering the Icelandic Basin on the eastern side of the Reykjanes Ridge (Dale et al., 2024).

The endmember of the Polar Surface Water ~~–~~ at the East Greenland Current ~~endmember (PSW-EGC~~(PSW_{EGC}, dark red diamond, Fig. 5) represents the ~~outflow surface waters in~~ surface water outflowing the Arctic Ocean at Fram Strait (Wefing et al., 2019), which are then transported south by the East Greenland Current (Fig. 1A). This endmember corresponds to ~~a sample~~ samples collected near the Denmark Strait in 2021 (St. MG17, Dale et al., 2024) and represents surface ~~waters~~ water entering the Labrador Sea via the West Greenland Current (WGC). As described in Dale et al. (2024) and Leist et al. (2024), ~~this sample is the~~ the samples most characteristic of ~~PSW-EGC in~~ PSW_{EGC} are located at the shelfbreak of southern Greenland, still containing a significant fraction of PSW (Dale et al., 2024)~~that outflows the Arctic Ocean (Wefing et al., 2025). The PSW-EGC~~ . The PSW_{EGC} endmember falls within a dilution line between NAC and the PSW sampled at 100 m depth in the Eurasian Basin (EB) in ~~the Central Arctic in~~ 2021 by Wefing et al. (2025) (grey circles, Fig. 5, Station Nr. 16, 28, 46 in Wefing et al. (2025)

). The ~~PSW-EGC and PSWfrom the central Arctic~~ PSW_{EGC} and PSW_{EB} from the Eurasian Basin both represent "younger" water imprinted with post-1980s reprocessing releases (Wefing et al., 2025) with high ^{129}I and comparably low ^{236}U- due to the shape of the input function of both tracers (Fig. A1).

In contrast, the "old" Arctic Atlantic Water (AAW) in the Arctic Canada Basin ~~at isopycnal σ_θ= 27.93 (AAW_{CB}, grey crosses~~(AAW_{CB}, grey diamond, Fig. 5), contains high ^{236}U and comparably low ^{129}I ~~(St. MK2, MK3 and CB29 in Payne et al., 2024) from~~ (Fram Strait Branch Water at St. MK2, MK3 and CB28b, CB29 in Payne et al., 2024). These tracer values correspond to global fallout and reprocessing discharges prior to the 1990s (Fig. A1). Above AAW_{CB}, the Pacific Summer Water holds especially low ^{129}I and ^{236}U from global fallout alone (dark green diamond in Fig. 5, all stations of JOIS 2020 Payne et al. (2024)). ~~We also include an endmember called Tracer free, which consists of sea ice and glacial meltwater, precipitation, and river runoff. Fresh water,~~

Freshwater, such as precipitation, river runoff, sea ice melt and glacial meltwater, is referred to as ~~Tracer-free~~ tracer-free and indicated as a diamond with a black outline in Fig. 5B. The Pacific Water, low in salinity, has only elevated ^{236}U from the global fallout, while the ~~WGIW~~NAC, even though its hydrographic properties are very different, has low tracer concentrations as well. Therefore, it is not possible to disentangle the different contributions of these water masses ~~. In future work, this might be addressed by adding~~ using ^{129}I and ^{236}U and one should add other tracers such as $\delta^{18}O$. Incorporating such an analysis, however, lies beyond the scope of this study, which focuses specifically on water masses identifiable through radionuclide signatures.

4.1.2 Geographical Endmembers in Nares Strait and Lancaster Sound

~~The measurements in Nares Strait and Lancaster Sound presented in this study provide suitable new endmembers for the northern exchange via these channels. They are represented in~~ Based on their geographic location, the 2024 measurements from western Nares Strait (unfilled orange symbols Fig. 5) and southern Lancaster Sound (unfilled red symbols) serve as geographical endmembers for characterising the inflows from the Arctic into Baffin Bay. The surface water at Nares Strait is characterised by low salinity (Fig. ~~5 as orange (Nares Strait)and red outlined symbols (Lancaster Sound). High tracer concentration observed below 200 m in ??~~B)and low tracer concentrations (Fig. 2A and B), both indicative of the inflow of tracer-free water (Münchow et al., 2006; Rabe et al., 2010). In northern Nares Strait ~~might reflect the mixture~~ (unfilled orange squares in Fig. 5) at depth below 200 m, high tracer signals were observed, probably as a result of the mixing between the Arctic-Atlantic ~~layer~~ waters from the Canada Basin (grey diamond ~~) and the central Arctic~~ in Fig. 5) and PSW originating from the Eurasian Basin, i.e. Amundsen and Makarov basins (grey circle ~~). On the contrary, low- and -at shallower depths may be due to inflowing Pacific Water.~~ in Fig. 5) (Münchow, Andreas et al., 2007; Jackson et al., 2014; Wefing et al., 2025).

In southern Nares Strait ~~, the observed tracer concentrations can be explained by mixing AAW~~ (unfilled orange circles in Fig. 5), downstream of the shallow 220 m sill, tracer concentrations observed below 150 m are consistent with a mixture of waters advected from northern Nares Strait~~with about 25% of Pacific Water or Tracer-free water. Samples from~~ , mixed with approximately 20% of tracer-free water, and potential contributions of water inflowing Nares Strait from eastern Baffin Bay

(Shroyer et al., 2015; Münchow, Andreas et al., 2007; Münchow, Andreas, and Humfrey Melling, 2008). This geographical endmember is illustrated as an orange cross in Fig. 5B), representing the inflowing waters to Baffin Bay.

Similar to Nares Strait, the surface water in southern Lancaster Sound (red ~~outlined~~ symbols in Fig. 5) ~~have generally lower tracer content than in Nares Strait~~is composed by Pacific and tracer-free water (Lehmann et al., 2022; McGeehan and Maslowski, 2012), as reflected by its low tracer concentration and salinity. However, ~~most~~ Lancaster Sound samples ~~appear to reflect a mixture of Arctic-Atlantic Waterin the Canada Basin (50–60%) with freshwater from the Pacific or Tracer-free water.~~ show a stronger influence from AAW_{CB}, as indicated by their position near the AAW_{CB} – Pacific Water mixing line. In 2024, the subsurface waters (10 m - 100 m) of western Lancaster Sound showed the highest AAW_{CB} contribution (55-65%) if mixing with Pacific Water. However, in Lancaster Sound, there is also a slight contribution of waters coming from Nares Strait (Lehmann et al., 2022; Shadwick, which circulate into Lancaster Sound. This is observed in two samples from 140 m and 200 m depth with tracer signals close to the NS_{South} endmember. Samples below 200 m from eastern Lancaster Sound (red unfilled diamonds in Fig. 5B) are strongly influenced by exchanges with Baffin Bay, indicated in temperature above 0°C (Fig. A2A), probably obtained by double-diffusion with WGIW (Lobb et al., 2003). For the geographical endmember (red cross in Fig. 5B), the station in western Lancaster Sound (red filled triangle) is selected, because it is considered to be more representative of the connectivity to the Arctic Canada Basin through the CAA. This endmember is calculated from the mean values in the upper 100 m, representative of the CAA outflow and thus excluding potential recirculation entering the Sound from Baffin Bay. However, it is important to note that samples taken in Lancaster Sound were collected two years after the samples in Davis Strait. Since outflow from Lancaster Sound is variable on interannual timescales (Prinsenberg and Hamilton, 2005), this endmember might not be fully representative of waters found in Baffin Bay. For example, in previous years, Lancanster Sound endmember might have had a stronger influence of AAW_{CB}, thus carrying a higher ^{236}U signal.

The presence of AAW_{CB} in central CAA has been previously observed using more detailed nutrients and temperature-salinity sampling (Jones et al., 2003; Rudels et al., 2004; Lehmann et al., 2022; Wang et al., 2012; Prinsenberg and Hamilton, 2005; Peterson et al. Despite the shallow passages through the CAA, the AAW_{CB} can make its way to Lancaster Sound as a result of the eastward transport by strong winds (Melling et al., 1984), tidal currents and vertical mixing enhanced by shallow bathymetry (Lehmann et al., 2022; Rudels, 1986; Hughes et al., 2017). The AAW_{CB} might further be upwelled to the Archipelago by easterly wind events (Peterson et al., 2012), associated with the Beaufort High or synoptic low-pressure systems originating in the North Pacific. This would result in upwelling of AAW_{CB} onto the shallow Chukchi and Beaufort Sea shelves, where AAW_{CB} can be transported towards the CAA as part of the Beaufort Sea shelfbreak jet (Pickart et al., 2013; Lin et al., 2019; Yang, 2006; Pickart et al., 2009. Although storms associated with AAW_{CB} upwelling are centred over the Aleutian Islands in the Bering Sea (Pickart et al., 2009), their northward passage into the Beaufort Sea can cause anomalies of cyclonic wind stress over the Canada Basin, which in turn increases volume transports through Lancaster Sound (Zhang et al., 2016; Peterson et al., 2012).

4.2 Evolution of West Greenland Shelf Water and West Greenland Irminger Water

West Greenland Shelf Water (WGSW) and West Greenland Irminger Water (WGIW) undergo strong seasonal hydrographic variability~~, with cooling and salinification~~. They cool and become more saline in winter and ~~freshening in summer(Curry et al., 2014)~~ freshen in summer, which complicates quantifying their role in water mass formation in ~~the~~ Baffin Bay (Curry et al., 2014). In contrast, radionuclide tracers remain unaffected by these processes, making them a powerful tool for tracking WGSW and WGIW in their journey to northern latitudes. In our dataset, the largest hydrographic variations are observed in WGSW: ~~in spring~~ samples from the AR7W Line show low temperatures ~~(~~in spring (overlapping dark red triangles in Fig. 4A), while autumn samples adjacent to Davis Strait display higher temperatures and a broad salinity range (all dark red symbols in Fig. 4A, with CT above 2°C). Despite these seasonal changes, tracer concentrations (Fig. 4B) remain remarkably stable, ~~allowing us to robustly quantify~~ enabling a robust quantification of the contribution of ~~the WGSW to Arctic Water formation. Using the binary mixing model, we find that the~~ WGSW ~~in~~ to water mass formation. In the model, mixing between PSW_{EGC} – NAC is considered in Fig. 6A for the formation and evolution of WGSW (dark red symbols) and WGIW (light green symbols).

Along the AR7W Line (dark red triangles in Fig. 6A~~as dark red triangles) retains~~) the WGSW retained up to 70% of the ~~PSW-EGC measured at Denmark Strait (fraction PSW-EGC = A/B, Fig. 6A, see Section 2.3 for fraction calculation).~~ PSW_{EGC}. As the WGSW flows ~~northwards~~ northward along the Greenland shelf, it becomes progressively entrained by tracer-free ~~waters~~ water and WGIW (light ~~blue~~ green symbols in Fig. 6A). By the time WGSW reaches ~~the Mooring and~~ Davis Strait and the Northern Line (diamonds and circles in Fig. 6A~~diamonds and circles~~), the ~~PSW-EGC fraction has decreased to about~~ PSW_{EGC} fraction has declined to approximately 40%~~, consistent with estimates of the thickness of the WGSW layer in the total water column by Huang et al. (2024) for southern Baffin Bay (160 m out of 600 m depth) and what Münchow et al. (2015) referred to as "anomalous waters" in the upper 800 m at the Greenland slope.~~ . This dilution could be compared to the decrease in the thickness of warm Polar Water (equivalent to WGSW) as they flow from eastern Davis Strait to eastern Northern Line, observed by Huang et al. (2024).

At central Baffin Bay, water classified as Arctic Water (~~teal square ,~~ light brown square in Fig. 6A), preserved a significant ~~PSW-EGC fraction of~~ fraction (about 30%~~. This was estimated as the fraction PSW-EGC = C/B, with the Arctic Water sample projected to the PSW-EGC-NAC mixing line in an extension of mixing with Transition Water~~) of PSW_{EGC} compared to the endmember at Denmark Strait. This finding contrasts with Huang et al. (2024) and Lehmann et al. (2022), who did not consider WGSW as a major contributor to the formation of water masses in the region. The substantial presence of WGSW may underscore the role of eddies, the off-branching character of the WGC, and the significant transformation of surface ~~waters~~ water in Baffin Bay. ~~WGIW (Fig. 6A light green symbols) lies~~

On the contrary, WGIW is positioned closer to the NAC endmember than WGSW, ~~because these waters have~~ reflecting a stronger influence from ~~waters coming directly from the south and thus have less tracer content~~southern-sourced water and thus exhibits lower tracer concentrations. An increase in its tracer content from the Labrador Sea to Baffin Bay confirms its mixing with WGSW, preserving approximately 15% ~~PSW-EGC (fraction PSW-EGC = 1-D/B)~~PSW_{EGC}, consistent with the decrease in the thisckness observed by Huang et al. (2024), while contrasting Rysgaard et al. (2020), who did not observe WGIW on the

Greenland shelf in Baffin Bay. Furthermore, Huang et al. (2024) observed ~~a 200 m thick WGIW layer, out of 500 m of the total water column,~~WGIW in central Baffin Bay, which could not be identified here, probably due to the limitation of the mixing of two endmembers in the tracer analysis.

4.3 Origin of Transition Water~~and~~ , Baffin Bay Mode and Bottom Water

The formation and origin of Transition Water ~~is a topic~~ (TrW) remain subjects of ongoing debate. ~~While Huang et al. (2024) described~~ Huang et al. (2024) characterised Transition Water (their TrW1) as a mixture of several water masses~~(~~, including WGIW, cold Arctic Water ~~, and WGSW), Rudels (2011) referred to~~ and WGSW. In contrast, Rudels (2011) described it as a blend of "Atlantic" water from the south and denser, colder northern water. ~~In T-S space (Fig. 4A), this formation is well supported by a mixture of cold Arctic Water with WGIW. However, the notably elevated concentrations of and low in Transition Wateralong the Northern Line (circles in Fig. 5A), Mooring Line (diamonds) and central Baffin Bay (squares) cannot be explained by mixing low- WGIW with intermediate- cold Arctic Water or WGSW with high concentrations of . This suggests that another endmember with more elevated must contribute to the formation~~ Complementing these perspectives, nutrient analyses by Lehmann et al. (2022) and Azetsu-Scott et al. (2010) identified WGIW, Pacific Water, and Arctic-Atlantic Waters as the primary contributors of Transition Water ~~. The only waters with such a high content are found in Nares Strait and Lancaster Sound (Fig. 5B). The AAW_{CB} outflowing Lancaster Sound meets this condition best when considering also the temperature and salinity of the Transition Water . To examine this further, we revisit Transition Water in~~ formation.

The broad range of ^{129}I~~-~~ and ^{236}U ~~space (dark blue symbols in Fig.~~ concentrations within Transition Water are consistent with the contribution from multiple endmembers (Huang et al., 2024; Lehmann et al., 2022). The temperature maximum within Transition Water (TrW_{Tmax}, dark blue symbol in Figs. 4 and 6A) ~~. A clear similarity emerges between Transition Water and waters from Lancaster Sound (red symbols~~ clusters near the Lancaster Sound endmember (red cross in Fig. 6A), ~~particularly those from its western part. These waters likely result from the dilution of AAW_{CB} by fresher (S_A<32) , low-tracer waters derived from the Pacific Ocean inflow, river runoff, and sea ice meltwater. Our observation of AAW_{CB} contrasts with most studies, which have typically considered Pacific-origin water as the main component of Arctic waters in the Baffin Bay (Goosse et al., 1997; Jones et al., 2003). None of these studies discusses the presence of AAWmaking its way through the Canadian Archipelago. This raises an important question: how can waters of Arctic-Atlantic origin, typically found below 200 m in the central Arctic Ocean, pass through the relatively shallow channels of the CAA? The estimated 40–45% contribution of AAW_{CB} to Transition Water formation (fraction AAW_{CB} = E/F, accounting for mixing~~ whereas the remaining Transition Water (light blue symbols in Figs. 4 and 6A) exhibits a spread towards lower temperatures and higher ^{129}I, indicative of additional mixing processes. However, as mentioned above, the Lancaster Sound outflow is known to be highly variable (Lehmann et al., 2022; Peterson et al., 2012; Prinsenberg and Hamilton, 2005) and might shift along the Pacific – AAW_{CB} mixing line. Therefore, the contribution of Lancaster Sound outflow to waters in Baffin Bay (TrW_{Tmax} and BBMW) is not calculated using this geographical endmember but from the mixing line between Pacific – AAW_{CB} endmembers. Although the Lancaster Sound outflow might not be considered as a fixed endmember, its influence remains apparent in the composition of Transition Water and TrW_{Tmax}. TrW_{Tmax} reflects contributions of cold, ^{236}U-rich AAW_{CB} mixed with Pacific Water ~~) and its presence~~

in from Lancaster Sound, is likely the result of upwelling in the Canada Basin. Easterly wind events, associated with the Beaufort High or synoptic low-pressure systems originating in the North Pacific, can result in the upwelling AAW_{CB} onto the shallow Chukchi and Beaufort Sea shelves, where AAW_{CB} can be transported towards the Canadian Arctic Archipelago as part of the Beaufort Sea shelfbreak jet (Pickart et al., 2013; Lin et al., 2019; Yang, 2006; Pickart et al., 2009). While storms associated with while its elevated temperatures are likely caused by mixing with warm, ^{129}I- and ^{236}U-poor WGIW within Baffin Bay. This results in a contribution of the AAW_{CB} upwelling are centred over the Allutian Islands in the Bering Sea (Pickart et al., 2009), as these storms travel northward into the Beaufort Sea, they can cause cyclonic wind stress anomalies over the Canada Basin, which in turn, increase volume transports through Lancaster Sound (Zhang et al., 2016; Peterson et al., 2012). These processes can drive the transport of denser shelf waters containing AAW_{CB} southward along the deeper passages of the CAA, such as M'Clintock Channel, eventually connecting to Lancaster Sound and northern Baffin Bay (Wang et al., 2012; Lehmann et al., . Once these mixed Pacific-AAW_{CB} shelf waters reach northwestern Baffin Bay, they can $_{CB}$ of 40–60% if calculated using Pacific water as the lower tracer endmember (i.e. this is a lower bound contribution, as TrW_{Tmax} also mix with WGIW). This finding aligns with observations by Lehmann et al. (2022), but emphasises the outflow of Lancaster Sound as more important than contributions by the Nares Strait endmember. This finding differs from Shadwick et al. (2011), who attributed the AAW component to Nares Strait outflow only. The Lancaster Sound outflow might be transported from shallow to intermediate depths by deep convection associated with large air-sea and cascading driven by intense air–sea fluxes and polynya development (Wang et al., 2012; Vincent, 2019; Yao and Tang, 2003; Aagaard and Carmack, 1989), and follow the strong activity (Wang et al., 2012; Vi , being subsequently redistributed through lateral exchange between the slope and basin waters, as modelled by e.g. Münchow et al. (2015) . From intermediate depthsin northern Baffin Bay, particularly at Münchow et al. (2015). At intermediate depths, particularly along the 27.5kg/m^3 isopycnal (~ 300 meters Lobb et al. (2003)), these dense waters can kg m^{-3} isopycnal (Lobb et al., 2003; Shan et al., , this dense water may encounter warm WGIW, where diffusive instability and cabbeling can cause these waters to further mix and descend in the water column promote further mixing and downward propagation (Lobb et al., 2003; Shan et al., 2024; Huang et al., 2024). In summary, while there is substantial physical uncertainty regarding the presence of AAW in the CAA, these processes provide a plausible mechanism for the high , forming TrW_{Tmax}.

Ultimately, Transition Water forms through the evolution of TrW_{Tmax} toward colder, fresher waters, which results in less ^{236}U concentrations within the watermass in central and southern Baffin Bay. The formation of Transition Water from only two main water masses (AAW, WGIW; Fig. 6A) contrasts with the interpretation by Huang et al. (2024) involving more water bodies. Further, by tracing its origin to Lancaster Sound and the Canada Basin, our findings add further detail to the broader framework proposed by Rudels (2011), in which Atlantic water of southern origin and dense northern water mix. Results further show that local hydrographic modifications described in literature (Curry et al., 2014; Tang et al., 2004; Shan et al., 2024; Melling et al., 2001) have no impact on the and higher ^{129}I and due to mixing with WGSW (Figure 6A, dashed line connecting TrW_{Tmax} with WGSW). WGSW may entrain Transition Water through cascading along the Greenland Shelf (Marson et al., 2017). Additionally, Transition Water might also have contributions from the Nares Strait outflow (Jones et al., 2003), as observed by the increased concentrations ^{236}U fingerprint. In the calculated AAW fraction, only mixing between AAW_{CB} and Pacific Water is taken into account, because the single contributions of WGIW vs.Pacific Water vs. Tracer-free Water can not be separated. Here,

the model is reaching its limitation since the water masses have low tracer concentrations, and the ratio between the tracers is too similar. The NAC endmember even aligns with the mixing between AAW_{CB} and Pacific Water. If one considers a main dilution by WGIW, our estimate of the AAW_{CB} fraction may be in the lower range.

Similar to that bring some of the Transition Water to the Nares Strait endmember in Fig. 6A.

Despite the limitations of a two-endmember model to constrain the origin and mixing of water masses, the radionuclide tracers strongly suggest the presence of AAW_{CB} outflowing Lancaster Sound and subsequently entraining Transition Water, a process that could not be quantified when using nutrient-based tracers alone (Lehmann et al., 2022; Azetsu-Scott et al., 2012). Furthermore, radionuclide tracers show negligible contributions of WGSW to TrW_{Tmax}.

Moving to greater depths, the origin and formation of BBMW still remain unclear (Bourke et al., 1989; Rudels et al., 2004). BBMW (purple symbols in Fig. 6A) remains unclear (Huang et al., 2024). BBMW has been suggested to be older than other water masses in the region, with tracer ages estimated to be up to 90 years (Lique et al., 2010)., which aligns well with a tracer signal of "old" water according to Fig. A1. The relatively high ^{236}U and very low ^{129}I displayed by BBMW may again indicate the presence of AAW_{CB}, and with the imprint of "old" waters, according to Fig. A1. These ages would agree with older AAW outflowing through the CAA, labelled with relatively elevated $_{CB}$ and align with observations by Rudels et al. (2004) and Bailey (1956). However, based on the available tracer data, it is not possible to differentiate if the AAW_{CB} originated from Nares Strait, as indicated by Rudels et al. (2004) and Bailey (1956) or from Lancaster Sound.

Finally, the deepest waters in Baffin Bay, also known as Baffin Bay Bottom Water (BBBW), remain tracer-free (Fig.4B, dark purple squares). Low tracer concentrations are consistent with observations by Bourke et al. (1989), which show that convection or cascading do not contribute to BBBW formation, and is further consistent with its long ventilation time of up to 455 years based on tritium and ^{3}He measurements (Top et al., 1980). Other studies have posited that Atlantic Water from the Canada Basin may contribute to BBBW formation (Rudels, 1986; Rudels et al., 2004), but this interpretation is incompatible with high tracer concentrations in the Canada Basin (Payne et al., 2024), which would manifest as elevated ^{129}I and almost no ^{236}U concentrations in BBBW.

4.4 Origin and formation of Arctic Water , and cold Arctic Waterand Transition Water mix

Arctic Water and cold Arctic Water are significant sources of freshwater to the subpolar North Atlantic, as and they are strongly influenced by sea iceand glacial meltwater (Huang et al., 2024; Curry et al., 2014; Shan et al., 2024), glacial meltwater and Pacific water (Huang et al., 2024; Sherwood et al., 2021; Curry et al., 2014; Shan et al., 2024). However, the composition of these freshwaters as they mix with other water masses in the region still remains under debate. The radionuclide tracers remains uncertain. Here, ^{236}U and ^{129}I demonstrate that cold Arctic Water is a mixture of Arctic Atlantic Arctic-Atlantic Water outflowing mostly through Nares Strait, Pacific Waters outflowing through the Canadian Archipelago and WGSWcoming from southern latitudesWater, and WGSW, with minor contributions from Lancaster Sound. Arctic Water has a similar origin, but with a stronger influence of tracer-free freshwater. In addition, the tracers reveal a distinct water mass, here termed Transition

~~Water mix, which has previously been grouped under Transition Water but appears to originate differently. Arctic Water (teal symbols)~~ Both Arctic Water and cold Arctic Water ~~(teal symbols with golden edges), as well as Transition Water mix (light blue), are shown~~ are presented in Fig. 6B ~~, alongside new endmembers, derived from the mean values of Transition Water and WGSW,~~ as light brown and teal symbols, respectively. The new endmember for WGSW is calculated as the mean of the values shown in Fig. 6A~~. Error bars indicate the standard deviation of the Transition Water and WGSW data points presented in the previous panel. For WGSW, the mean and standard deviation were derived from~~ , with the error bars representing the corresponding standard deviation. This endmember includes all samples with concentrations of ^{129}I ~~concentration~~ below 240×10^{7} ~~at~~ atoms/kg~~to best represent~~ , selected to best characterise the core of WGSW ~~reaching north of~~ advecting north beyond Davis Strait. We consider mixing between Lancaster Sound (to best represent the surface and subsurface inflow) and WGSW (Lehmann et al., 2022); Nares Strait outflow (NS_{South}) and Pacific Waters (Jackson et al., 2014). Additionally, potential mixing between Lancaster Sound and NAC and WGSW with NAC (Marson et al., 2017) is indicated as grey solid lines.

Cold Arctic Water ~~has~~ generally has higher tracer concentrations than Arctic Water and is confined to a cold (CT ~~about~~ ~ -1.5 °C) and rather narrow temperature range, while it covers a salinity range between 32.5 and 33.6 (~~Fig~~Figs. 4 and ~~A2~~**??**). Although Huang et al. (2024) observed mixing between cold ~~Polar Water (similar to this study cold Arctic~~ Arctic Water (their cold Polar Water), ~~Meteoric Water, as well as WGIW, the mixing model here~~ meteoric water, and WGIW, our mixing model (Fig. 6B) points to additional ~~waters contributing to~~ water masses involved in its formation. In the following, we examine each ~~of them~~ contributor in detail, starting with WGSW.

In the binary mixing ~~plot~~model, cold Arctic Water ~~(Fig. 6B, teal symbols with golden edges)~~ stretches from the mixing line of Nares Strait South (NS~~South~~$_{South}$) and Pacific Water towards the endmember of WGSW, suggesting the ~~influence of WGSW on~~ presence of WGSW in cold Arctic Water as well. The largest contribution of WGSW, approximately ~~65~~80%, is observed in a sample ~~at a depth of~~ located at 54 m depth in the middle of the Northern Line ~~as indicated~~ (circle in Fig. 6B)~~by an "a", and the fraction WGSW = G/H~~. WGSW generally follows the main cyclonic circulation (Curry et al., 2011; Azetsu-Scott et al., 2012; Huang et al., 2024)~~and~~ , which may cool through air-sea heat exchange ~~,~~ in winter (especially in the North Water ~~polynya in winter,~~ Polynya) and cascade along the Greenland shelf (Marson et al., 2017), thus reaching the temperature of the cold Arctic Water (Yao and Tang, 2003). ~~AAW (fraction AAW=I/J), probably outflowing through Nares Strait ,~~ In central Baffin Bay (teal square in Fig. 6B), the Nares Strait outflow contributes up to ~~35~~70% to cold Arctic Water~~("b" in Fig. 6B). The role of the outflow of Nares Strait, previously observed by Huang et al. (2024) and Melling et al. (2001), is now reinforced based on a completely different set of tracers.~~ , in agreement with previous observations by Huang et al. (2024); Lehmann et al. (2022) and Melling et al. (2001).

Finally, Pacific Water and ~~WGIW, both characterised by~~ NAC (Fig. 6B) with low ^{129}I and ^{236}U may contribute to cold Arctic Water as well. While Huang et al. (2024) focused primarily on contributions of WGIW, the radionuclide tracer data is less conclusive, as mixing with either source produces a similar low-tracer signal~~("c" in Fig. 6B).~~ . At this stage, the binary mixing model reaches its limit, unable to distinguish between these two low-tracer endmembers. Finally, mixing with Arctic Water, as previously noted by Huang et al. (2024), is likely but cannot be precisely quantified here due to similar ^{129}I and

^{236}U signatures of cold Arctic Water and Arctic Water. Overall, the cold Arctic Water cluster reflects a varying blend of water masses described above, showing no ~~clear trend in hydrographic properties .~~ such clear trend when looking at hydrographic properties only.

Following the assessment of the cold Arctic Water cluster, we turn to Arctic Water to explore its distinct properties and its close association with cold Arctic Water~~in tracer space~~. Although Arctic Water is fresher than cold Arctic Water, both water masses plot closely together in tracer space (~~teal~~ light brown and teal symbols in Fig. 6B). Arctic Water appears to be the result of ~~the dilution of~~ similar sources as cold Arctic Water ~~with~~ but with higher contributions of low-tracer ~~waters~~water, probably of ~~Tracer-free~~ tracer-free and Pacific origin ~~(Huang et al., 2024; Planat et al., 2025). Unlike cold~~ (Huang et al., 2024; Planat et al., 2025; Shery . In Arctic Water, ~~Arctic Water shows the strongest WGSW influence~~ contributions of WGSW are observed in central Baffin Bay (light brown square in Fig. 6B), highlighting the strong stratification in this region. ~~The input of low tracer water, similar to that in cold Arctic Water, is most pronounced along the western side~~ On the western flank of the Northern Line~~("d" ,~~ there is an influx of low tracer water (light brown circles in Fig. 6B), probably due to mixing with 50% of Pacific Water (if mixing between Pacific and NS_{South} is considered). These mixed waters remain confined within the BIC and are transported southward. Stronger mixing with cold Arctic Water likely occurs near ~~the Mooring Line~~Davis Strait (diamond symbols), illustrating the dynamic conditions in this area (Huang et al., 2024; Tang et al., 2004). Further south in the Northern Labrador Sea Line (~~stars~~star symbols), Arctic Water was likely sampled within the bifurcation of the WGC, showing ~~up to 30% WGSW ("e" in Fig. 6B, fraction WGSW = K/L, "e" projected onto line "L" parallel to line "H")~~a WGSW contribution of up to 70% (if mixing with Lancaster Sound outflow is considered). Gou et al. (2022) attributed a southward transport of water confined to the Greenland Coast to an instability of the WGC, which leads to shedding eddies in the northern Labrador Sea. In comparison, at the AR7W Line (triangles), Arctic Water carried by the Labrador Current ~~primarily transports the AAW tracer signalwith up to 30%contribution when mixing of NSSouth~~ transports a lower ^{129}I signal, probably originating from the Nares Strait outflow (up to 70%, again if mixing NS_{South} with Pacific Water is considered~~("f" in)~~. As the Labrador Current continues southward along the Canada Shelf, two surface samples (red triangles Fig. 6B~~, fraction AAW=M~~) originating south west of the AR7W Line suggest further mixing between WGSW, Nares Strait and/~~J~~or Lancaster Sound outflow and a low tracer component, probably of North Atlantic origin (i.e. NAC). The ~~transition from a predominantly WGSW endmember to AAW — potentially sourced from Nares Strait— remains unresolved based on the current data.~~two surface samples are warmer (CT: 1.5°C) and more saline (S_A: 33.8) than Arctic Water, but colder and fresher than the remaining samples classified as Labrador Sea surface (Fig.4). Possible influences on the main water masses observed in the Labrador Current might ~~be caused by the~~ include: seasonal variability in ~~the southward velocities observed~~ southward velocities at Davis Strait, which are generally highest in summer and lowest in winter (Curry et al., 2014; Myers, 2005; Shan et al., 2024)~~or~~ ; variability in the outflow of AAW_{CB} ~~CB~~ via Hudson Strait ~~,~~ south of the Northern Labrador Sea Line (Straneo and Saucier, 2008)~~. Water classified as Transition Water mix bridges Transition Water and cold Arctic Water in TS and tracer space (light blue in Fig. 4 and 6B) and may represent the mixing and cooling of AAW_{CB} from Lancaster Sound and /or Nares Strait and WGSW. Here, the binary mixing model is less conclusive about the origin of AAW, since mixing with WGSW would spread AAW_{CB} from Lancaster Sound towards~~

the ratios observed for AAW outflowing Nares Strait. Therefore, AAW originating from either Lancaster Sound or Nares Strait needs to be considered. ; the presence of eddies and Irminger Rings (Gou et al., 2022).

4.5 Implications on the formation of Labrador Sea Water and North East Atlantic Deep Water

The formation of Labrador Sea Water (LSW) is governed by complex driven by deep winter convection and associated physical processes (Clarke and Gascard, 1983)and influenced by various , and is modulated by multiple freshwater sources (salinity <<34.6PSU, Zhang et al. (2021a)) that can impact ; Zhang et al. 2021a) that alter its properties (Yashayaev, 2007; Yamamoto-Kawai et al., 2008). To date, the The relative contributions of these freshwater sources remain unresolvedsources remain uncertain, with most studies focusing on boundary inputs freshwater inputs from boundary currents (Schmidt and Send, 2007; Zhang et al., 2021a). In contrast, artificial radionuclides reveal the potential significance of off-boundary sources , such as Transition Water and Baffin Bay Mode Water, not only for LSW formation but also for the highlight the potential importance of off-boundary current sources in the formation of both LSW and North East Atlantic Deep Water (NEADW). Insights from ^{129}I and ^{236}U tracers suggest that the properties of LSW and NEADW may be shaped by mixing between BBMW, Transition Water (TrW), and the North Atlantic Current (NAC).

In the previous study by Leist et al. (2024) using ^{129}I and ^{236}U in the Labrador Sea region, the mixing model reached its limitations when trying to understand the origin of LSW, due to low tracer concentrations and the absence of critical endmembers. However, the study identified Nonetheless, that study showed that ^{129}I rich WGSW eddies as one of the sources contributing -rich WGSW eddies contribute to LSW as they branch off the WGC and move into the interior of the Labrador Sea (Leist et al., 2024; Hátún et al., 2007; Holliday et al., 2009; Lilly et al., 2003; Chanut et al., 2008; Pacini and Pickart, 2022). Labrador Sea Water (red blue symbols in Fig. 6C) appear appears to have a significant contribution of WGSW, estimated here to be up to 20% (WGSW fraction = N/L30% (if mixing with the NAC endmember is considered). The influence on surface waters in the Labrador Sea (dark orange in Fig. 6C) is even higherof WGSW is even stronger, up to 40%(WGSW fraction = O/L, crossing point of surface sample with mixing line estimated along the linear regression between all surface samples).Another water mass that might contribute to the tracer load in LSW is DSOW, as previously discussed in Dale et al. (2024) and Leist et al. (2024) . The formation of DSOW north of the Denmark Strait is complex and discussed in greater detail by Dale et al. (2024) and Tanhua et al. (2005). One possible source of DSOW is a branch of the EGC carrying water of Arctic origin outflowing via Fram Strait, which ultimately contributes to the deep overflow at the Denmark Strait. During this convection process, it can already mix with LSW, present in the Irminger Sea, and circulate within the subpolar gyre (Lavender et al., 2005; Zou et al., 2023). Once at the Labrador Sea , DSOW is confined to the bottom of the basin and separated from LSW by NEADW. However, tracer similarities between surface samples and DSOW were still observed in the Labrador Sea in 2022. See for example the two AR7W surface samples in 70%, on surface water of the eastern Labrador Sea (light red triangles in Fig. 6C(highlighted by "g"), which fall within the DSOW cluster, despite differences in their temperature and salinity properties (Fig. 4, colder (CT <1.5°C) and fresher (S_A <34) compared to the other surface samples) and located close to the WGC at the AR7W Line.).

Another source of ^{129}I and ^{236}U in the LSW could be the Labrador Current, carrying Arctic Water and cold Arctic Water, but this would contributions to the LSW formation might be relatively small (< 10%), as already discussed in Myers (2005); Pickart and Spall (

previously discussed in Myers (2005), Pickart and Spall (2007), Wang et al. (2018) and Duyck et al. (2025). However, the main LSW cluster observed in Fig. 6C (~~red triangles) appears to have shifted to the left of the mixing line between the DSOW cluster and NAC~~blue triangles) is located at comparable low ^{129}I and elevated ^{236}U concentrations. This suggests that another water mass, richer in ^{236}U relative to ^{129}I, is required to account for the observed composition of LSW. This feature, first noted ~~in 2014~~ by Castrillejo et al. (2018) and later confirmed by Leist et al. (2024), can now be explained by the influence of ~~Transition Water, which flows out of~~ the Transition Water outflowing Davis Strait and ~~entrains~~ entraining into LSW. ~~Among the water masses~~

Among the southward-flowing water entering the Labrador Sea, the Transition Water is the only ~~one~~ watermass with sufficiently high ^{236}U concentrations to explain the tracer signature of LSW. To our knowledge, this entrainment of ~~Transition Water~~ the Transition Water outflowing Baffin Bay into LSW has not been previously considered in the literature. To estimate the contributions of Transition Water a new endmember is derived from the maximum temperature observed in Transition Water (TrW_{Tmax}, dark blue cross in Fig. 6C) with error bars reflecting the variability between samples. As shown by ~~"h"~~ the blue triangles in Fig. 6C, ~~this contribution~~ the contribution of TrW_{Tmax} could be as high as ~~30%(fraction TrW = P/Q)~~20%. In Davis Strait, long-term moored measurements of temperature and salinity ~~,~~ (Fig. A2A, B), and across-strait velocity ~~from~~ (2004-2024) at 60°W and 500 ~~meters at the Mooring Line support this argument and show that Transition Water flows southward~~ m depth support this view (Fig. A2C). They show a persistent southward flow of Transition Water from Davis Strait ~~year-round~~ into the Labrador Sea ~~(Fig. A2)~~from 2004 to 2024, complementing gridded transports for the 2004-2010 period (Curry et al., 2014). These measurements ~~are located near~~ coincide with the ^{236}U maximum in ~~the Mooring Line~~ Davis Strait (^{236}U$\sim$ 17.5 $\times 10^6$ at/kg, Fig. 3)~~and demonstrate the consistent interannually southward transport of waters~~ , demonstrating that the transport towards the Labrador Sea of water fresher than LSW ($S_A < 34.9$ g/kg) ~~into the Labrador Sea, providing~~ provides both a ^{236}U and freshwater source for LSW. Once the Transition Water enters the Labrador Sea, it may ~~become~~ be entrained with LSW ~~throughout the year through cross-density mixing , as observed by Zou et al. (2020)in southern Labrador and the Irminger Sea~~through mixing along-density surfaces Zou et al. (2020). Furthermore, similar concentrations of ^{129}I and ^{236}U between BBMW and LSW (Fig. 4) suggest that substantial mixing also occurs between these water masses. ~~With an average salinity~~ As a result, with an average $S_A <$ of 34.49 g/kg, BBMW can also act as a further freshwater source ~~to~~ for LSW. These previously unreported freshwater contributions ~~to LSW~~ from Transition Water and BBMW to LSW can help shed light on potentially unresolved physical processes in ocean models that contribute to deep convection variability in the Labrador Sea.

Finally, NEADW is a water mass that originates from multiple sources, including ISOW ~~, DSOW,~~ and LSW (Yashayaev, 2007; García-Ibáñez et al., 2015). In the mixing model (yellow triangles in Fig. 6C), NEADW occupies a low-tracer area influenced by several of these ~~sources.~~ water sources, and known to be strongly entrained by ISOW (yellow-green diamond Fig. 6C, from Dale et al. (2024)) while the contribution of DSOW (dark green triangles) is minor (García-Ibáñez et al., 2018) . However, the elevated ~~^{236}U relative to ^{129}I~~ ^{236}U relative to ^{129}I is not explained by the endmembers established so far. Our results suggest that Transition Water and/or BBMW contribute up to ~~30~~25% to NEADW ~~, with the remaining from NAC waters~~when mixing with NAC is considered. During autumn and winter, BBMW ~~may~~ can enter the deep Labrador Sea as a

weak overflow through Davis Strait (Huang et al., 2024; Curry et al., 2014)~~and join this deeper layer in the Labrador Sea, thus mixing~~. Once there, it joins the deeper layers and mixes with NEADW. Although the simple two-endmember model used here cannot fully resolve every ~~water mass contribution~~contribution, particularly under low tracer concentrations and multiple sources, it still provides a valuable first-order approximation. Future work could build on this foundation with a more comprehensive multiparameter analysis.

5 Conclusions

~~By applying~~ This study uses ^{129}I and ^{236}U ~~as~~ tracers in Baffin Bay, Davis Strait, and the Labrador Sea ~~, this study provides new constraints on~~ to better resolve the pathways and transformations of Arctic and Atlantic ~~waters~~water. Elevated ^{236}U in Transition Water reveals that Arctic–Atlantic Water from the Canada Basin contributes significantly ~~to its~~ (up to 60%) to Transition Water formation, demonstrating that the outflow of Atlantic-derived ~~waters~~water, most probably through Lancaster Sound, has been underestimated so far. At the same time, our results show that the West Greenland Shelf ~~Waters feed into Arctic Waters~~ Water feeds into Arctic Water (75%) in central Baffin Bay~~, while cold Arctic Waters largely originate from Nares Strait and mixes with~~. Cold Arctic Water is influenced by Nares Strait outflow (up to 70%) at the centre of the bay, while on the eastern side, it contains up to 80% West Greenland Shelf ~~water~~Water. These processes highlight the role of Arctic outflows in the delivery of freshwater to Baffin Bay and ~~further south~~the Labrador Sea. South of Davis Strait, our results show that Transition Water provides a ~~substantial contribution to~~ notable contribution (up to 20%) to the formation of Labrador Sea Water ~~and~~ with potential contributions to North East Atlantic Deep Water. This previously ~~unrecognised~~ overlooked pathway not only supplies freshwater but also leaves a distinct tracer signature, with direct implications for convection processes in the Labrador Sea and the composition of North East Atlantic Deep Water.

Together, these findings emphasise that Arctic outflows through the Canadian Arctic Archipelago are more important than previously assumed. They shape the transformation of Baffin Bay water masses and exert a significant influence on the ventilation and freshwater budget of the subpolar North Atlantic. ~~Capturing~~ This work motivates repeated sampling to understand inter-annual variability, while capturing these processes more accurately in ocean models will be essential for predicting future changes in deep water formation and the stability of the Atlantic Meridional Overturning Circulation.

Data availability. The original datasets for this study can be found at the Zenodo database (https://doi.org/10.5281/zenodo.16914587). The CTD data of Lancaster Sound and Nares Strait are provided by Amundsen Science Data Collection Amundsen Science Data Collection (2024).

Author contributions. LGTL, MC and NC contributed to the conception and design of the study. LGTL performed the data investigation, formal analysis, and wrote the original draft of the manuscript. The investigation and formal analysis were supported by NC and MC. JL contributed substantially to the interpretation of the results. HT, CV and NC performed AMS measurements. NC and MC supervised the

study. NC and LGTL acquired funding. KAS, CL and MR supported sample collection during expeditions and provided hydrographic data. All authors contributed to the manuscript revision and approved the submitted version.

Competing interests. The authors declare that the research was without a conflict of interest.

Acknowledgements. The PI Núria Casacuberta has received funding from the European Research Council (ERC) under the European Union's Horizon 2020 research and innovation programme (TITANICA project, ERC2020-COG 101001451) and from the Swiss National Science Foundation (PR00P2-193091-TRACEATLANTIC). In addition, Lisa Leist received funding from the Swiss Polar Institute (Polar Access Fund, PAF-2022-03). Jed Lenetsky received funding from the U.S. National Science Foundation awards 1902628 and 1902595. KAS is funded through the OFSI fund, Davis Strait Observing System, by Fisheries and Oceans Canada. Maxi ~~Castrilejo~~ Castrillejo acknowledges funding from the Swiss National Science Foundation project CARVICE (2000021E_214835). The authors acknowledge the chief scientists, the captains and the crew of the R/V Neil Armstrong and the R/V Atlantis. The scientists involved in the sampling are deeply acknowledged. The authors also thank Emmy Hieronimus~~and Catherine Jeandel~~, who collected the samples at Lancaster Sound ~~and Nares Strait onbord~~ aboard of CCGS Amundsen. Kayley Kündig and Simona Staub are thanked for their contributions to ETH-based laboratories. In addition, the authors acknowledge the entire ASOF community and their contribution through various discussions. Maps were created using cartopy and the GEBCO data product.

References

Aagaard, K. and Carmack, E. C.: The role of sea ice and other fresh water in the Arctic circulation, Journal of Geophysical Research: Oceans, 94, 14 485–14 498, https://doi.org/10.1029/jc094ic10p14485, publisher: American Geophysical Union (AGU), 1989.

Amundsen Science Data Collection: 2024. CTD-Rosette data collected by the CCGS Amundsen in the Canadian Arctic, Processed data. Version [version]. Archived at www.polardata.ca, Canadian Cryospheric Information Network (CCIN), Waterloo, Canada. doi: 10.5884/12713. Accessed on 06.11.2025, 2024.

Azetsu-Scott, K., Clarke, A., Falkner, K., Hamilton, J., Jones, E. P., Lee, C., Petrie, B., Prinsenberg, S., Starr, M., and Yeats, P.: Calcium carbonate saturation states in the waters of the Canadian Arctic Archipelago and the Labrador Sea, Journal of Geophysical Research: Oceans, 115, 2009JC005 917, https://doi.org/10.1029/2009JC005917, 2010.

Azetsu-Scott, K., Petrie, B., Yeats, P., and Lee, C.: Composition and fluxes of freshwater through Davis Strait using multiple chemical tracers, J. Geophys. Res., 117, 2012JC008 172, https://doi.org/10.1029/2012JC008172, 2012.

Bailey, W. B.: On the Origin of Deep Baffin Bay Water, Journal of the Fisheries Research Board of Canada, 13, 303–308, https://doi.org/10.1139/f56-020, 1956.

Bamber, J. L., Tedstone, A. J., King, M. D., Howat, I. M., Enderlin, E. M., Van Den Broeke, M. R., and Noel, B.: Land Ice Freshwater Budget of the Arctic and North Atlantic Oceans: 1. Data, Methods, and Results, Journal of Geophysical Research: Oceans, 123, 1827–1837, https://doi.org/10.1002/2017JC013605, 2018.

Bourke, R. H., Addison, V. G., and Paquette, R. G.: Oceanography of Nares Strait and northern Baffin Bay in 1986 with emphasis on deep and bottom water formation, J. Geophys. Res., 94, 8289–8302, https://doi.org/10.1029/JC094iC06p08289, 1989.

Bower, A. S., Lozier, M. S., Gary, S. F., and Böning, C. W.: Interior pathways of the North Atlantic meridional overturning circulation, Nature, 459, 243–247, https://doi.org/10.1038/nature07979, 2009.

Boyd, P. W., Claustre, H., Levy, M., Siegel, D. A., and Weber, T.: Multi-faceted particle pumps drive carbon sequestration in the ocean, Nature, 568, 327–335, https://doi.org/10.1038/s41586-019-1098-2, publisher: Springer Science and Business Media LLC, 2019.

Carmack, E. C., Yamamoto-Kawai, M., Haine, T. W. N., Bacon, S., Bluhm, B. A., Lique, C., Melling, H., Polyakov, I. V., Straneo, F., Timmermans, M., and Williams, W. J.: Freshwater and its role in the Arctic Marine System: Sources, disposition, storage, export, and physical and biogeochemical consequences in the Arctic and global oceans, Journal of Geophysical Research: Biogeosciences, 121, 675–717, https://doi.org/10.1002/2015jg003140, publisher: American Geophysical Union (AGU), 2016.

Casacuberta, N. and Smith, J. N.: Nuclear Reprocessing Tracers Illuminate Flow Features and Connectivity Between the Arctic and Subpolar North Atlantic Oceans, Annual Review of Marine Science, 15, 203–221, https://doi.org/10.1146/annurev-marine-032122-112413, 2023.

Casacuberta, N., Masqué, P., Henderson, G., Rutgers van-der Loeff, M., Bauch, D., Vockenhuber, C., Daraoui, A., Walther, C., Synal, H.-A., and Christl, M.: First 236U data from the Arctic Ocean and use of 236U/238U and 129I/236U as a new dual tracer, Earth and Planetary Science Letters, 440, 127–134, https://doi.org/10.1016/j.epsl.2016.02.020, 2016.

Castrillejo, M., Casacuberta, N., Christl, M., Vockenhuber, C., Synal, H.-A., García-Ibáñez, M. I., Lherminier, P., Sarthou, G., Garcia-Orellana, J., and Masqué, P.: Tracing water masses with \textbackslashchem^129I and \textbackslashchem^236U in the subpolar North Atlantic along the GEOTRACES GA01 section, Biogeosciences, 15, 5545–5564, https://doi.org/10.5194/bg-15-5545-2018, 2018.

Chanut, J., Barnier, B., Large, W., Debreu, L., Penduff, T., Molines, J. M., and Mathiot, P.: Mesoscale Eddies in the Labrador Sea and Their Contribution to Convection and Restratification, Journal of Physical Oceanography, 38, 1617–1643, https://doi.org/10.1175/2008JPO3485.1, 2008.

Christl, M., Vockenhuber, C., Kubik, P., Wacker, L., Lachner, J., Alfimov, V., and Synal, H.-A.: The ETH Zurich AMS facilities: Performance parameters and reference materials, Nuclear Instruments and Methods in Physics Research Section B: Beam Interactions with Materials and Atoms, 294, 29–38, https://doi.org/10.1016/j.nimb.2012.03.004, 2013.

Christl, M., Casacuberta, N., Vockenhuber, C., Elsässer, C., Bailly du Bois, P., Herrmann, J., and Synal, H.: Reconstruction of the ^{236}U input function for the Northeast Atlantic Ocean: Implications for ^{129}I/^{236}U and ^{236}U/^{238}U-based tracer ages, Journal of Geophysical Research: Oceans, 120, 7282–7299, https://doi.org/10.1002/2015JC011116, 2015.

Christl, M., Gautschi, P., Maxeiner, S., Müller, A. M., Vockenhuber, C., and Synal, H.-A.: 236U analyses with the ETH Zurich MILEA prototype system, Nuclear Instruments and Methods in Physics Research Section B: Beam Interactions with Materials and Atoms, 534, 61–71, https://doi.org/10.1016/j.nimb.2022.11.009, 2023.

Clarke, R. A. and Gascard, J.-C.: The Formation of Labrador Sea Water. Part I: Large-Scale Processes, Journal of Physical Oceanography, 13, 1764 – 1778, https://doi.org/https://doi.org/10.1175/1520-0485(1983)013<1764:TFOLSW>2.0.CO;2, 1983.

Cuny, J., Rhines, P. B., Niiler, P. P., and Bacon, S.: Labrador Sea Boundary Currents and the Fate of the Irminger Sea Water, Journal of Physical Oceanography, 32, 627–647, https://doi.org/10.1175/1520-0485(2002)032<0627:LSBCAT>2.0.CO;2, 2002.

Cuny, J., Rhines, P. B., and Ron Kwok: Davis Strait volume, freshwater and heat fluxes, Deep Sea Research Part I: Oceanographic Research Papers, 52, 519–542, https://doi.org/10.1016/j.dsr.2004.10.006, 2005.

Curry, B., Lee, C. M., and Petrie, B.: Volume, Freshwater, and Heat Fluxes through Davis Strait, 2004–05*, Journal of Physical Oceanography, 41, 429–436, https://doi.org/10.1175/2010JPO4536.1, 2011.

Curry, B., Lee, C. M., Petrie, B., Moritz, R. E., and Kwok, R.: Multiyear Volume, Liquid Freshwater, and Sea Ice Transports through Davis Strait, 2004–10, Journal of Physical Oceanography, 44, 1244 – 1266, https://doi.org/10.1175/JPO-D-13-0177.1, 2014.

Dale, D., Christl, M., Vockenhuber, C., Macrander, A., Ólafsdóttir, S., Middag, R., and Casacuberta, N.: Tracing Ocean Circulation and Mixing From the Arctic to the Subpolar North Atlantic Using the ^{129}I– ^{236}U Dual Tracer, JGR Oceans, 129, e2024JC021 211, https://doi.org/10.1029/2024JC021211, 2024.

Dickson, R. R. and Brown, J.: The production of North Atlantic Deep Water: Sources, rates, and pathways, Journal of Geophysical Research: Oceans, 99, 12 319–12 341, https://doi.org/10.1029/94JC00530, 1994.

Dunlap, E. and Tang, C. C.: Modelling the Mean Circulation of Baffin Bay, Atmosphere-Ocean, 44, 99–109, https://doi.org/10.3137/ao.440107, 2006.

Duyck, E., Foukal, N. P., and Frajka-Williams, E.: Circulation of Baffin Bay and Hudson Bay waters on the Labrador shelf and into the subpolar North Atlantic, Ocean Science, 21, 241–260, https://doi.org/10.5194/os-21-241-2025, 2025.

García-Ibáñez, M. I., Pardo, P. C., Carracedo, L. I., Mercier, H., Lherminier, P., Ríos, A. F., and Pérez, F. F.: Structure, transports and transformations of the water masses in the Atlantic Subpolar Gyre, Progress in Oceanography, 135, 18–36, https://doi.org/10.1016/j.pocean.2015.03.009, 2015.

García-Ibáñez, M. I., Pérez, F. F., Lherminier, P., Zunino, P., Mercier, H., and Tréguer, P.: Water mass distributions and transports for the 2014 GEOVIDE cruise in the North Atlantic, Biogeosciences, 15, 2075–2090, https://doi.org/10.5194/bg-15-2075-2018, 2018.

Gardner, A. S., Moholdt, G., Wouters, B., Wolken, G. J., Burgess, D. O., Sharp, M. J., Cogley, J. G., Braun, C., and Labine, C.: Sharply increased mass loss from glaciers and ice caps in the Canadian Arctic Archipelago, Nature, 473, 357–360, https://doi.org/10.1038/nature10089, 2011.

Gelderloos, R., Katsman, C. A., and Drijfhout, S. S.: Assessing the Roles of Three Eddy Types in Restratifying the Labrador Sea after Deep Convection, Journal of Physical Oceanography, 41, 2102–2119, https://doi.org/10.1175/JPO-D-11-054.1, 2011.

Goosse, H., Fichefet, T., and Campin, J.-M.: The effects of the water flow through the Canadian Archipelago in a global ice-ocean model, Geophysical Research Letters, 24, 1507–1510, https://doi.org/https://doi.org/10.1029/97GL01352, 1997.

Gou, R., Pennelly, C., and Myers, P. G.: The Changing Behavior of the West Greenland Current System in a Very High-Resolution Model, Journal of Geophysical Research: Oceans, 127, https://doi.org/10.1029/2022JC018404, 2022.

Grenier, M., Brown, K., Colombo, M., Belhadj, M., Baconnais, I., Pham, V., Soon, M., Myers, P., Jeandel, C., and François, R.: Controlling factors and impacts of river-borne neodymium isotope signatures and rare earth element concentrations supplied to the Canadian Arctic Archipelago, Earth and Planetary Science Letters, 578, 117 341, https://doi.org/10.1016/j.epsl.2021.117341, 2022.

Haine, T. W., Curry, B., Gerdes, R., Hansen, E., Karcher, M., Lee, C., Rudels, B., Spreen, G., De Steur, L., Stewart, K. D., and Woodgate, R.: Arctic freshwater export: Status, mechanisms, and prospects, Global and Planetary Change, 125, 13–35, https://doi.org/10.1016/j.gloplacha.2014.11.013, publisher: Elsevier BV, 2015.

Holland, D. M., Thomas, R. H., De Young, B., Ribergaard, M. H., and Lyberth, B.: Acceleration of Jakobshavn Isbræ triggered by warm subsurface ocean waters, Nature Geoscience, 1, 659–664, https://doi.org/10.1038/ngeo316, publisher: Springer Science and Business Media LLC, 2008.

Holliday, N. P., Bacon, S., Allen, J., and McDonagh, E. L.: Circulation and Transport in the Western Boundary Currents at Cape Farewell, Greenland, Journal of Physical Oceanography, 39, 1854–1870, https://doi.org/10.1175/2009JPO4160.1, 2009.

Huang, J., Pickart, R. S., Bahr, F., McRaven, L. T., Tremblay, J.-R., Michel, C., Jeansson, E., Kopec, B., Welker, J. M., and Ólafsdóttir, S. R.: Water mass evolution and general circulation of Baffin Bay: Observations from two shipboard surveys in 2021, Progress in Oceanography, 229, 103 322, https://doi.org/10.1016/j.pocean.2024.103322, 2024.

Hughes, K. G., Klymak, J. M., Hu, X., and Myers, P. G.: Water mass modification and mixing rates in a 1/12° simulation of the Canadian Arctic Archipelago: MIXING IN THE CANADIAN ARCHIPELAGO, Journal of Geophysical Research: Oceans, 122, 803–820, https://doi.org/10.1002/2016JC012235, 2017.

Hátún, H., Eriksen, C. C., and Rhines, P. B.: Buoyant Eddies Entering the Labrador Sea Observed with Gliders and Altimetry, Journal of Physical Oceanography, 37, 2838–2854, https://doi.org/10.1175/2007JPO3567.1, 2007.

IOC, S. and IAPSO: The international thermodynamic equation of seawater - 2010: Calculation and use of thermodynamic properties., Intergovernmental Oceanographic Commission, Manuals and Guides No. 56, UNESCO (English), 196 pp., https://www.teos-10.org/pubs/gsw/html/gsw_CT_from_t.html, 2010.

Jackson, J. M., Lique, C., Alkire, M., Steele, M., Lee, C. M., Smethie, W. M., and Schlosser, P.: On the waters upstream of Nares Strait, Arctic Ocean, from 1991 to 2012, Continental Shelf Research, 73, 83–96, https://doi.org/10.1016/j.csr.2013.11.025, 2014.

Jones, E. P., Swift, J. H., Anderson, L. G., Lipizer, M., Civitarese, G., Falkner, K. K., Kattner, G., and McLaughlin, F.: Tracing Pacific water in the North Atlantic Ocean, Journal of Geophysical Research: Oceans, 108, https://doi.org/https://doi.org/10.1029/2001JC001141, 2003.

Komuro, Y. and Hasumi, H.: Intensification of the Atlantic Deep Circulation by the Canadian Archipelago Throughflow, Journal of Physical Oceanography, 35, 775–789, https://doi.org/10.1175/JPO2709.1, 2005.

Lavender, K. L., Brechner Owens, W., and Davis, R. E.: The mid-depth circulation of the subpolar North Atlantic Ocean as measured by subsurface floats, Deep Sea Research Part I: Oceanographic Research Papers, 52, 767–785, https://doi.org/10.1016/j.dsr.2004.12.007, 2005.

Le Bras, I. A.-A.: Labrador sea water spreading and the Atlantic meridional overturning circulation, Philosophical Transactions of the Royal Society A: Mathematical, Physical and Engineering Sciences, 381, 20220 189, https://doi.org/10.1098/rsta.2022.0189, 2023.

Lehmann, N., Kienast, M., Granger, J., Bourbonnais, A., Altabet, M. A., and Tremblay, J.: Remote Western Arctic Nutrients Fuel Remineralization in Deep Baffin Bay, Global Biogeochemical Cycles, 33, 649–667, https://doi.org/10.1029/2018GB006134, 2019.

Lehmann, N., Kienast, M., Granger, J., and Tremblay, J.: Physical and Biogeochemical Influences on Nutrients Through the Canadian Arctic Archipelago: Insights From Nitrate Isotope Ratios, Journal of Geophysical Research: Oceans, 127, e2021JC018 179, https://doi.org/10.1029/2021JC018179, 2022.

Leist, L. G. T., Castrillejo, M., Smith, J. N., Christl, M., Vockenhuber, C., Velo, A., Lherminier, P., and Casacuberta, N.: 129I and 236U distribution in the subpolar North Atlantic unravels water mass provenance in AR7W and A25 lines, Frontiers in Marine Science, 11, 1470 675, https://doi.org/10.3389/fmars.2024.1470675, 2024.

Li, J., Pickart, R. S., Lin, P., Bahr, F., Arrigo, K. R., Juranek, L., and Yang, X.: The Atlantic Water Boundary Current in the Chukchi Borderland and Southern Canada Basin, Journal of Geophysical Research: Oceans, 125, e2020JC016 197, https://doi.org/10.1029/2020JC016197, 2020.

Lilly, J. M., Rhines, P. B., Schott, F., Lavender, K., Lazier, J., Send, U., and D'Asaro, E.: Observations of the Labrador Sea eddy field, Progress in Oceanography, 59, 75–176, https://doi.org/10.1016/j.pocean.2003.08.013, 2003.

Lin, P., Pickart, R. S., Torres, D. J., and Pacini, A.: Evolution of the Freshwater Coastal Current at the Southern Tip of Greenland, Journal of Physical Oceanography, 48, 2127–2140, https://doi.org/10.1175/JPO-D-18-0035.1, 2018.

Lin, P., Pickart, R. S., Moore, G., Spall, M. A., and Hu, J.: Characteristics and dynamics of wind-driven upwelling in the Alaskan Beaufort Sea based on six years of mooring data, Deep Sea Research Part II: Topical Studies in Oceanography, 162, 79–92, https://doi.org/10.1016/j.dsr2.2018.01.002, publisher: Elsevier BV, 2019.

Lique, C., Treguier, A. M., Blanke, B., and Grima, N.: On the origins of water masses exported along both sides of Greenland: A Lagrangian model analysis, Journal of Geophysical Research: Oceans, 115, https://doi.org/https://doi.org/10.1029/2009JC005316, 2010.

Lobb, J., Carmack, E. C., Ingram, R. G., and Weaver, A. J.: Structure and mixing across an Arctic/Atlantic front in northern Baffin Bay, Geophysical Research Letters, 30, 2003GL017 755, https://doi.org/10.1029/2003GL017755, 2003.

Lozier, M. S.: Overturning in the subpolar North Atlantic: a review, Philosophical Transactions of the Royal Society A: Mathematical, Physical and Engineering Sciences, 381, 20220 191, https://doi.org/10.1098/rsta.2022.0191, 2023.

Malles, J.-H., Marzeion, B., and Myers, P. G.: Freshwater input from glacier melt outside Greenland alters modeled northern high-latitude ocean circulation, Earth System Dynamics, 16, 347–377, https://doi.org/10.5194/esd-16-347-2025, 2025.

Marson, J. M., Myers, P. G., Hu, X., Petrie, B., Azetsu-Scott, K., and Lee, C. M.: Cascading off the W est G reenland S helf: A numerical perspective, Journal of Geophysical Research: Oceans, 122, 5316–5328, https://doi.org/10.1002/2017JC012801, 2017.

McGeehan, T. and Maslowski, W.: Evaluation and control mechanisms of volume and freshwater export through the Canadian Arctic Archipelago in a high-resolution pan-Arctic ice-ocean model, Journal of Geophysical Research: Oceans, 117, 2011JC007 261, https://doi.org/10.1029/2011JC007261, 2012.

Melling, H., Lake, R., Topham, D., and Fissel, D.: Oceanic thermal structure in the western Canadian Arctic, Continental Shelf Research, 3, 233–258, https://doi.org/10.1016/0278-4343(84)90010-4, 1984.

Melling, H., Gratton, Y., and Ingram, G.: Ocean circulation within the North Water polynya of Baffin Bay, Atmosphere-Ocean, 39, 301–325, https://doi.org/10.1080/07055900.2001.9649683, 2001.

Melling, H., Agnew, T. A., Falkner, K. K., Greenberg, D. A., Lee, C. M., Münchow, A., et al.: Fresh-water fluxes via Pacific and Arctic outflows across the Canadian polar shelf, in: Arctic–Subarctic Ocean Fluxes: Defining the Role of the Northern Seas in Climate, edited by Dickson, R. R., Meincke, J., and Rhines, P., pp. 193–247, Springer, 2008.

Myers, P. G.: Impact of freshwater from the Canadian Arctic Archipelago on Labrador Sea Water formation, Geophys. Res. Lett., 32, L06 605, https://doi.org/10.1029/2004GL022082, 2005.

Myers, P. G., Donnelly, C., and Ribergaard, M. H.: Structure and variability of the West Greenland Current in Summer derived from 6 repeat standard sections, Progress in Oceanography, 80, 93–112, https://doi.org/10.1016/j.pocean.2008.12.003, 2009.

Münchow, A., Melling, H., and Falkner, K. K.: An Observational Estimate of Volume and Freshwater Flux Leaving the Arctic Ocean through Nares Strait, Journal of Physical Oceanography, 36, 2025–2041, https://doi.org/10.1175/JPO2962.1, 2006.

Münchow, A., Falkner, K. K., and Melling, H.: Baffin Island and West Greenland Current Systems in northern Baffin Bay, Progress in Oceanography, 132, 305–317, https://doi.org/10.1016/j.pocean.2014.04.001, 2015.

Münchow, Andreas, Falkner, K.K., and Humfrey Melling: Spatial continuity of measured seawater and tracer fluxes through Nares Strait, a dynamically wide channel bordering the Canadian Archipelago, Journal of Marine Research, 65, 759–788, 2007.

Münchow, Andreas, and Humfrey Melling: Ocean current observations from Nares Strait to the west of Greenland: Interannual to tidal variability and forcing, Journal of Marine Research, 66, https://elischolar.library.yale.edu/journal_of_marine_research/216, 2008.

Pacini, A. and Pickart, R. S.: Meanders of the West Greenland Current near Cape Farewell, Deep Sea Research Part I: Oceanographic Research Papers, 179, 103 664, https://doi.org/10.1016/j.dsr.2021.103664, 2022.

Payne, A.: Anthropogenic Radionuclides as Tracers of Transport, Mixing, Carbon Storage and Freshwater sources in the Canadian Arctic Ocean, Ph.D. thesis, ETH Zurich, 2026.

Payne, A., Wefing, A., Christl, M., Vockenhuber, C., Williams, W., Smith, J. N., and Casacuberta, N.: Circulation Timescales and Pathways of Atlantic Water in the Canada Basin: Insights From Transient Tracers ^{129} I and ^{236} U, Journal of Geophysical Research: Oceans, 129, e2023JC020 813, https://doi.org/10.1029/2023JC020813, 2024.

Pelle, T., Myers, P. G., Hamilton, A., Mazloff, M., Soderlund, K., Beem, L., Blankenship, D. D., Grima, C., Habbal, F., Skidmore, M., and Greenbaum, J. S.: Ocean circulation, sea ice, and productivity simulated in Jones Sound, Canadian Arctic Archipelago, between 2003–2016, EGUsphere, 2024, 1–34, https://doi.org/10.5194/egusphere-2024-3751, 2024.

Peterson, I., Hamilton, J., Prinsenberg, S., and Pettipas, R.: Wind-forcing of volume transport through Lancaster Sound, Journal of Geophysical Research: Oceans, 117, https://doi.org/https://doi.org/10.1029/2012JC008140, 2012.

Pickart, R. S. and Spall, M. A.: Impact of Labrador Sea Convection on the North Atlantic Meridional Overturning Circulation, Journal of Physical Oceanography, 37, 2207–2227, https://doi.org/10.1175/JPO3178.1, 2007.

Pickart, R. S., Moore, G. W. K., Torres, D. J., Fratantoni, P. S., Goldsmith, R. A., and Yang, J.: Upwelling on the continental slope of the Alaskan Beaufort Sea: Storms, ice, and oceanographic response, Journal of Geophysical Research: Oceans, 114, https://doi.org/10.1029/2008jc005009, publisher: American Geophysical Union (AGU), 2009.

Pickart, R. S., Spall, M. A., and Mathis, J. T.: Dynamics of upwelling in the Alaskan Beaufort Sea and associated shelf–basin fluxes, Deep Sea Research Part I: Oceanographic Research Papers, 76, 35–51, https://doi.org/10.1016/j.dsr.2013.01.007, 2013.

Planat, N., Tremblay, L. B., Dufour, C. O., and Straub, D.: Seasonal and Decadal Geostrophic Pathways of Pacific and Atlantic Waters in the Arctic Amerasian Basin From Observations, Journal of Geophysical Research: Oceans, 130, e2024JC021 560, https://doi.org/10.1029/2024JC021560, 2025.

Polyakov, I. V., Pnyushkov, A. V., Alkire, M. B., Ashik, I. M., Baumann, T. M., Carmack, E. C., Goszczko, I., Guthrie, J., Ivanov, V. V., Kanzow, T., Krishfield, R., Kwok, R., Sundfjord, A., Morison, J., Rember, R., and Yulin, A.: Greater role for Atlantic inflows on sea-ice loss in the Eurasian Basin of the Arctic Ocean, Science, 356, 285–291, https://doi.org/10.1126/science.aai8204, 2017.

Polyakov, I. V., Pnyushkov, A. V., Charette, M., Cho, K.-H., Jung, J., Kipp, L., Muilwijk, M., Whitmore, L., Yang, E. J., and Yoo, J.: Atlantification advances into the Amerasian Basin of the Arctic Ocean, Science Advances, 11, eadq7580, https://doi.org/10.1126/sciadv.adq7580, 2025.

Prinsenberg, S. and Hamilton, J.: Monitoring the volume, freshwater and heat fluxes passing through Lancaster sound in the Canadian arctic archipelago, Atmosphere-Ocean, 43, 1–22, https://doi.org/10.3137/ao.430101, 2005.

Rabe, B., Münchow, A., Johnson, H. L., and Melling, H.: Nares Strait hydrography and salinity field from a 3-year moored array, Journal of Geophysical Research: Oceans, 115, 2009JC005 966, https://doi.org/10.1029/2009JC005966, 2010.

Rantanen, M., Karpechko, A. Y., Lipponen, A., Nordling, K., Hyvärinen, O., Ruosteenoja, K., Vihma, T., and Laaksonen, A.: The Arctic has warmed nearly four times faster than the globe since 1979, Communications Earth & Environment, 3, 168, https://doi.org/10.1038/s43247-022-00498-3, 2022.

Rhein, M., Steinfeldt, R., Kieke, D., Stendardo, I., and Yashayaev, I.: Ventilation variability of Labrador Sea Water and its impact on oxygen and anthropogenic carbon: a review, Philosophical Transactions of the Royal Society A: Mathematical, Physical and Engineering Sciences, 375, 20160 321, https://doi.org/10.1098/rsta.2016.0321, 2017.

Rudels, B.: The outflow of polar water through the Arctic Archipelago and the oceanographic conditions in Baffin Bay, Polar Research, 4, 161–180, https://doi.org/10.1111/j.1751-8369.1986.tb00528.x, 1986.

Rudels, B.: Volume and freshwater transports through the Canadian Arctic Archipelago–Baffin Bay system, Journal of Geophysical Research, 116, C00D10, https://doi.org/10.1029/2011JC007019, 2011.

Rudels, B., Jones, E. P., Anderson, L. G., and Kattner, G.: On the Intermediate Depth Waters of the Arctic Ocean, in: Geophysical Monograph Series, edited by Johannessen, O. M., Muench, R. D., and Overland, J. E., pp. 33–46, American Geophysical Union, ISBN 978-1-118-66388-2 978-0-87590-042-1, https://doi.org/10.1029/GM085p0033, 1994.

Rudels, B., Jones, E. P., Schauer, U., and Eriksson, P.: Atlantic sources of the Arctic Ocean surface and halocline waters, Polar Research, 23, 181–208, https://doi.org/10.3402/polar.v23i2.6278, 2004.

Rysgaard, S., Boone, W., Carlson, D., Sejr, M. K., Bendtsen, J., Juul-Pedersen, T., Lund, H., Meire, L., and Mortensen, J.: An Updated View on Water Masses on the pan-West Greenland Continental Shelf and Their Link to Proglacial Fjords, J. Geophys. Res. Oceans, 125, https://doi.org/10.1029/2019JC015564, 2020.

Schmidt, S. and Send, U.: Origin and Composition of Seasonal Labrador Sea Freshwater, Journal of Physical Oceanography, 37, 1445–1454, https://doi.org/10.1175/JPO3065.1, 2007.

Shadwick, E., Thomas, H., Gratton, Y., Leong, D., Moore, S., Papakyriakou, T., and Prowe, A.: Export of Pacific carbon through the Arctic Archipelago to the North Atlantic, Continental Shelf Research, 31, 806–816, https://doi.org/10.1016/j.csr.2011.01.014, 2011.

Shan, X., Spall, M. A., Pennelly, C., and Myers, P. G.: Seasonal Variability in Baffin Bay, Journal of Geophysical Research: Oceans, 129, e2024JC021 038, https://doi.org/https://doi.org/10.1029/2024JC021038, e2024JC021038 2024JC021038, 2024.

Sherwood, O. A., Davin, S. H., Lehmann, N., Buchwald, C., Edinger, E. N., Lehmann, M. F., and Kienast, M.: Stable isotope ratios in seawater nitrate reflect the influence of Pacific water along the northwest Atlantic margin, Biogeosciences, 18, 4491–4510, https://doi.org/10.5194/bg-18-4491-2021, 2021.

Shroyer, E. L., Samelson, R. M., Padman, L., and Münchow, A.: Modeled ocean circulation in N ares S trait and its dependence on landfast-ice cover, Journal of Geophysical Research: Oceans, 120, 7934–7959, https://doi.org/10.1002/2015JC011091, 2015.

Straneo, F. and Saucier, F.: The outflow from Hudson Strait and its contribution to the Labrador Current, Deep Sea Research Part I: Oceanographic Research Papers, 55, 926–946, https://doi.org/https://doi.org/10.1016/j.dsr.2008.03.012, 2008.

Sutherland, D. A., Pickart, R. S., Peter Jones, E., Azetsu-Scott, K., Jane Eert, A., and Ólafsson, J.: Freshwater composition of the waters off southeast Greenland and their link to the Arctic Ocean, Journal of Geophysical Research, 114, C05 020, https://doi.org/10.1029/2008JC004808, 2009.

Tang, C. C., Ross, C. K., Yao, T., Petrie, B., DeTracey, B. M., and Dunlap, E.: The circulation, water masses and sea-ice of Baffin Bay, Progress in Oceanography, 63, 183–228, https://doi.org/10.1016/j.pocean.2004.09.005, 2004.

Tanhua, T.: Spreading of overflow water from the Greenland to the Labrador Sea, Geophys. Res. Lett., 32, L10 605, https://doi.org/10.1029/2005GL022700, 2005.

Tanhua, T., Olsson, K. A., and Jeansson, E.: Formation of Denmark Strait overflow water and its hydro-chemical composition, Journal of Marine Systems, 57, 264–288, https://doi.org/10.1016/j.jmarsys.2005.05.003, 2005.

The IMBIE Team: Mass balance of the Greenland Ice Sheet from 1992 to 2018, Nature, 579, 233–239, https://doi.org/10.1038/s41586-019-1855-2, 2020.

Top, Z., Clarke, W. B., Eismont, W. C., and Jones, E. P.: Radiogenic helium in Baffin Bay bottom water, Journal of Marine Research, 38, 435–452, https://elischolar.library.yale.edu/journal_of_marine_research/1514, 1980.

Vandecrux, B., Fausto, R. S., Box, J. E., Covi, F., Hock, R., Rennermalm, A. K., Heilig, A., Abermann, J., Van As, D., Bjerre, E., Fettweis, X., Smeets, P. C. J. P., Kuipers Munneke, P., Van Den Broeke, M. R., Brils, M., Langen, P. L., Mottram, R., and Ahlstrom, A. P.: Recent warming trends of the Greenland ice sheet documented by historical firn and ice temperature observations and machine learning, The Cryosphere, 18, 609–631, https://doi.org/10.5194/tc-18-609-2024, 2024.

Vincent, R. F.: A Study of the North Water Polynya Ice Arch using Four Decades of Satellite Data, Scientific Reports, 9, 20 278, https://doi.org/10.1038/s41598-019-56780-6, 2019.

Vockenhuber, C., Casacuberta, N., Christl, M., and Synal, H.-A.: Accelerator Mass Spectrometry of 129I towards its lower limits, Nuclear Instruments and Methods in Physics Research Section B: Beam Interactions with Materials and Atoms, 361, 445–449, https://doi.org/10.1016/j.nimb.2015.01.061, 2015.

Wang, H., Legg, S., and Hallberg, R.: The Effect of Arctic Freshwater Pathways on North Atlantic Convection and the Atlantic Meridional Overturning Circulation, J. Climate, 31, 5165–5188, https://doi.org/10.1175/JCLI-D-17-0629.1, 2018.

Wang, Q., Myers, P. G., Hu, X., and Bush, A. B.: Flow Constraints on Pathways through the Canadian Arctic Archipelago, Atmosphere-Ocean, 50, 373–385, https://doi.org/10.1080/07055900.2012.704348, 2012.

Wang, Q., Shu, Q., Wang, S., Beszczynska-Moeller, A., Danilov, S., Steur, L., Haine, T. W. N., Karcher, M., Lee, C. M., Myers, P. G., Polyakov, I. V., Provost, C., Skagseth, t., Spreen, G., and Woodgate, R.: A Review of Arctic–Subarctic Ocean Linkages: Past Changes, Mechanisms, and Future Projections, Ocean-Land-Atmos Res, 2, 0013, https://doi.org/10.34133/olar.0013, 2023.

Wang, Q., Shu, Q., and Wang, F.: Recent emergence of Arctic atlantification dominated by climate warming, Science Advances, 10, eadq5235, https://doi.org/10.1126/sciadv.adq5235, 2024.

Wefing, A., Christl, M., Vockenhuber, C., Rutgers van der Loeff, M., and Casacuberta, N.: Tracing Atlantic Waters Using ^{129}236$ U in the Fram Strait in 2016, Journal of Geophysical Research: Oceans, 124, 882–896, https://doi.org/10.1029/2018JC014399, 2019.

Wefing, A.-M., Casacuberta, N., Christl, M., Gruber, N., and Smith, J. N.: Circulation timescales of Atlantic Water in the Arctic Ocean determined from anthropogenic radionuclides, Ocean Science, 17, 111–129, https://doi.org/10.5194/os-17-111-2021, 2021.

Wefing, A.-M., Payne, A., Scheiwiller, M., Vockenhuber, C., Christl, M., Tanhua, T., and Casacuberta, N.: Changes in Atlantic Water circulation in the central Arctic Ocean between 2011 and 2021 inferred from tracer observations, EGUsphere, pp. 1–44, https://doi.org/10.5194/egusphere-2025-1322, 2025.

Weijer, W., Haine, T. W. N., Siddiqui, A. H., Cheng, W., Veneziani, M., and Kurtakoti, P.: INTERACTIONS BETWEEN THE ARCTIC MEDITERRANEAN AND THE ATLANTIC MERIDIONAL OVERTURNING CIRCULATION: A REVIEW, Oceanography, 35(3/4), 118–127, https://www.jstor.org/stable/27182704, 2022.

Yamamoto-Kawai, M., McLaughlin, F. A., Carmack, E. C., Nishino, S., and Shimada, K.: Freshwater budget of the Canada Basin, Arctic Ocean, from salinity, δ^{18} O, and nutrients, Journal of Geophysical Research: Oceans, 113, 2006JC003 858, https://doi.org/10.1029/2006JC003858, 2008.

Yang, J.: The Seasonal Variability of the Arctic Ocean Ekman Transport and Its Role in the Mixed Layer Heat and Salt Fluxes, Journal of Climate, 19, 5366–5387, https://doi.org/10.1175/jcli3892.1, publisher: American Meteorological Society, 2006.

Yao, T. and Tang, C. L.: The formation and maintenance of the North Water Polynya, Atmosphere-Ocean, 41, 187–201, https://doi.org/10.3137/ao.410301, 2003.

Yashayaev, I.: Changing freshwater content: Insights from the subpolar North Atlantic and new oceanographic challenges, Progress in Oceanography, 73, 203–209, https://doi.org/10.1016/j.pocean.2007.04.014, 2007.

Yashayaev, I.: Intensification and shutdown of deep convection in the Labrador Sea were caused by changes in atmospheric and freshwater dynamics, Communications Earth & Environment, 5, 156, https://doi.org/10.1038/s43247-024-01296-9, 2024.

Zhang, J., Weijer, W., Steele, M., Cheng, W., Verma, T., and Veneziani, M.: Labrador Sea freshening linked to Beaufort Gyre freshwater release, Nature Communications, 12, 1229, https://doi.org/10.1038/s41467-021-21470-3, 2021a.

Zhang, Y., Chen, C., Beardsley, R. C., Gao, G., Lai, Z., Curry, B., Lee, C. M., Lin, H., Qi, J., and Xu, Q.: Studies of the Canadian Arctic Archipelago water transport and its relationship to basin-local forcings: Results from AO-FVCOM, Journal of Geophysical Research: Oceans, 121, 4392–4415, https://doi.org/10.1002/2016JC011634, 2016.

Zhang, Y., Chen, C.-S., Shen, X.-Y., Xu, D.-Y., Shao, W.-Z., Beardsley, R. C., Chang, L., and Feng, G.-P.: Role of sea level pressure in variations of the Canadian Arctic Archipelago throughflow, Advances in Climate Change Research, 12, 539–552, https://doi.org/10.1016/j.accre.2021.07.009, 2021b.

Zou, S., Lozier, M. S., Li, F., Abernathey, R., and Jackson, L.: Density-compensated overturning in the Labrador Sea, Nature Geoscience, 13, 121–126, https://doi.org/10.1038/s41561-019-0517-1, 2020.

Zou, S., Bower, A. S., Lozier, M. S., and Furey, H. H.: Deep ocean circulation in the subpolar North Atlantic observed by acoustically-tracked floats, Progress in Oceanography, 211, 102 975, https://doi.org/10.1016/j.pocean.2023.102975, 2023.

Zou, S., Petit, T., Li, F., and Lozier, M. S.: Observation-Based Estimates of Water Mass Transformation and Formation in the Labrador Sea, Journal of Physical Oceanography, 54, 1411–1429, https://doi.org/10.1175/JPO-D-23-0235.1, 2024.

Zweng, M. M. and Münchow, A.: Warming and freshening of Baffin Bay, 1916–2003, Journal of Geophysical Research: Oceans, 111, 2005JC003 093, https://doi.org/10.1029/2005JC003093, 2006.

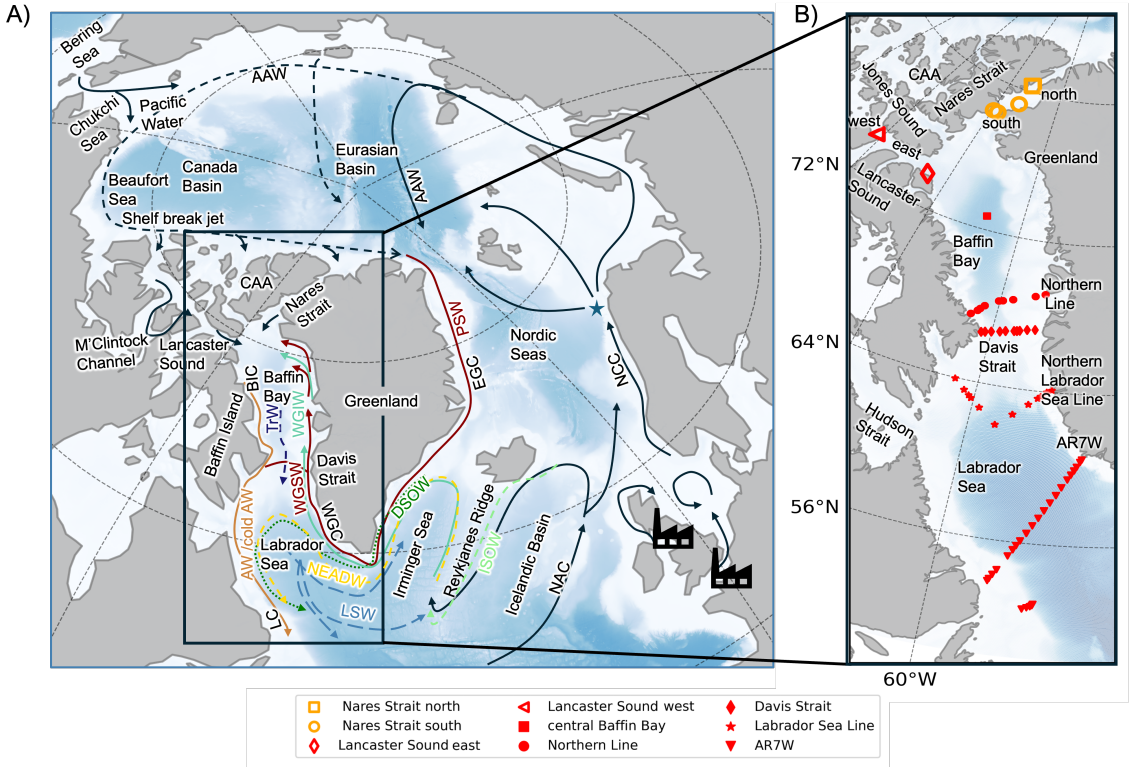

Figure 1. A) Map of the study area showing the main surface water mass circulation as solid lines, intermediate-depth circulation as dashed lines, and deep circulation as dotted lines, adapted from Curry et al. (2014), García-Ibáñez et al. (2015) and ~~Dale et al. (2024)~~ Dale et al. (2024). ~~The ocean~~ Ocean current names are ~~stated~~ shown in black ~~text~~font, while specific water mass names are ~~in~~ represented in ~~colors~~other colours. Black icons ~~mark~~ indicate the locations of ~~the~~ nuclear fuel reprocessing plants at Sellafield (UK) and La Hague (France), and the blue star marks the location where the tracers input function is defined (Fig. A1). **B)** Close-up view highlighting regional geographic ~~details~~ features and the oceanographic transects sampled in this study~~, indicated by distinct~~. Filled red symbols indicate sampling locations surrounding Davis Strait and along AR7W in 2022: central Baffin Bay (square), Northern Line (dots), Davis Strait (diamonds), Northern Labrador Sea Line (stars), and AR7W (triangles). Unfilled red symbols represent samples from Lancaster Sound (west: triangle, east: diamond), while unfilled orange symbols represent samples from Nares Strait (north: square, south: circles). All ~~acronyms~~ abbreviations are defined in Appendix Table A1.

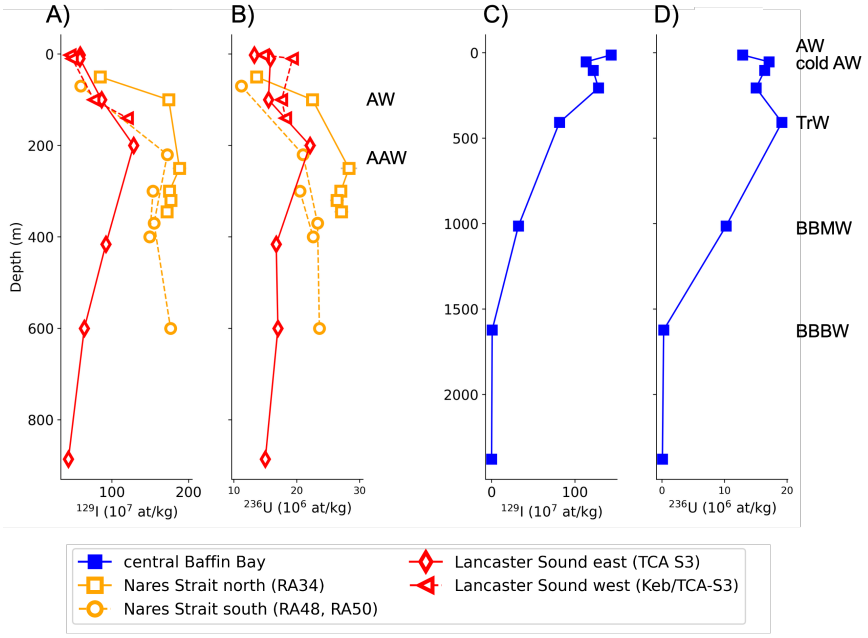

Figure 2. ~~A) Concentrations of~~ Concentration depth profiles in Nares Strait (orange) and Lancaster Sound (red) ~~profiles. B~~for ^{129}I (**A**) ~~Concentrations of~~ and ^{236}U ~~in Nares Strait and Lancaster Sound; C~~(**B**). ^{129}I ~~concentrations in the Central Baffin Bay station and D~~(**C**) ~~Concentration of~~ and ^{236}U (**D**) depth profiles in ~~the Central~~ central Baffin Bay~~Station~~.

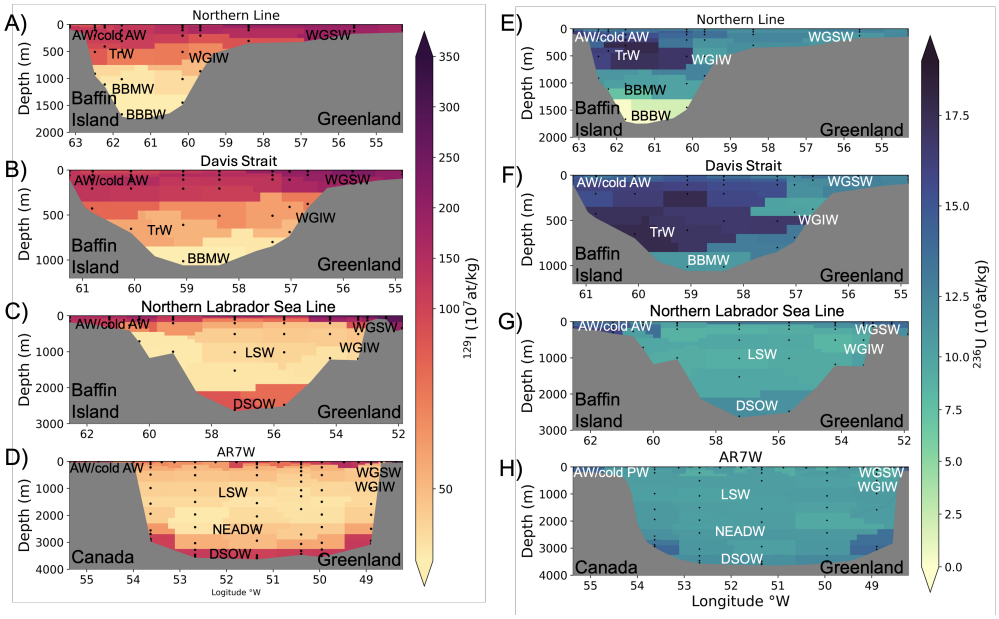

Figure 3. Zonal distribution of ^{129}I (~~A-D~~A – D) and ^{236}U concentrations (~~E-H~~E – H) along Northern Line (**A, E**), ~~Mooring Line~~ Davis Strait (**B, F**), Northern ~~Larador~~ Labrador Sea Line (**C, G**) and AR7W (**D, H**), respectively, in 2022. The water masses are based on ~~Curry et al. (2014); Yashayaev (2007); Huang et al. (2024)~~Curry et al. (2014), Yashayaev (2007), and Huang et al. (2024).

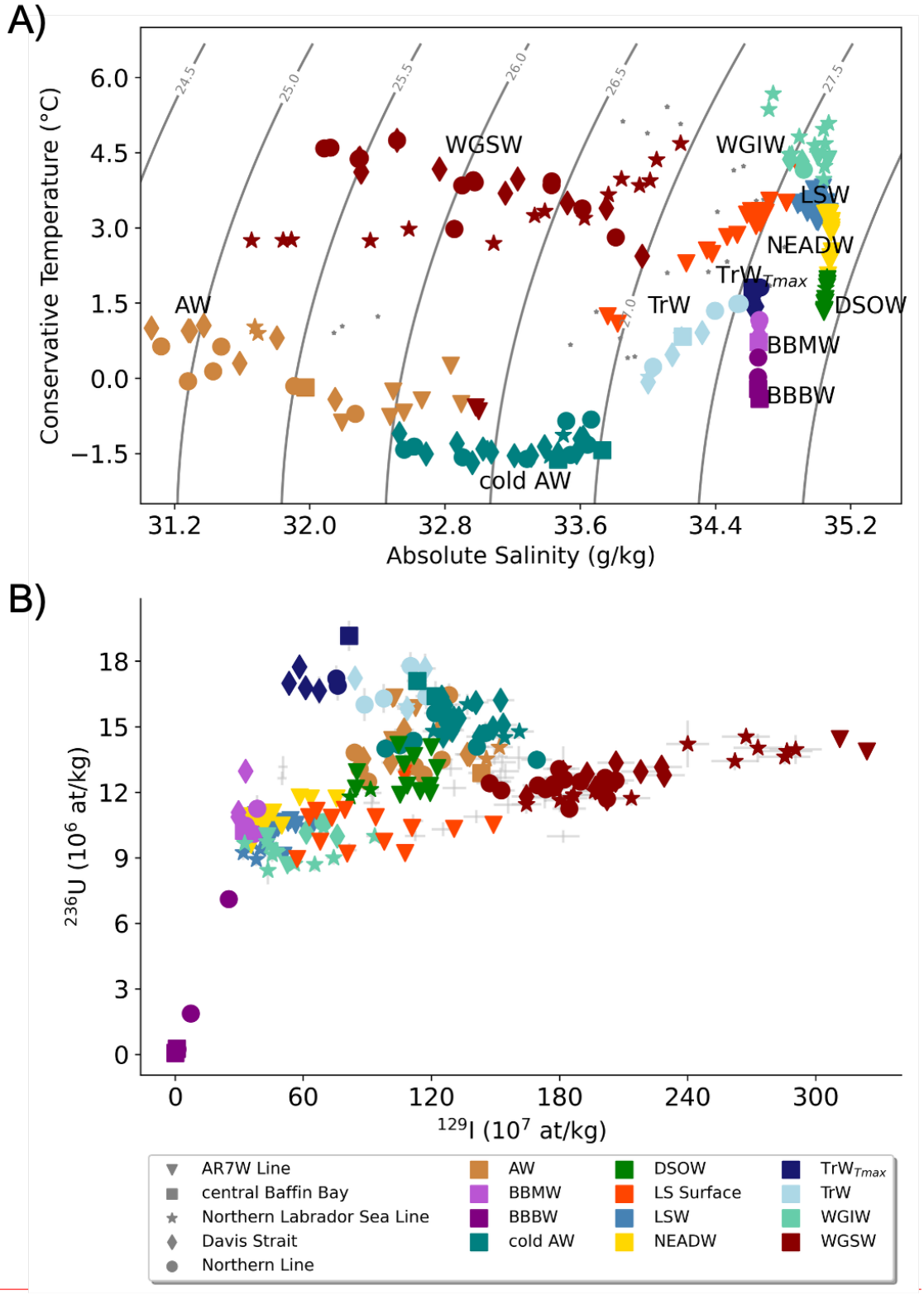
A)
Conservative Temperature (°C)
Absolute Salinity (g/kg)
24.5
25.0
25.5
26.0
26.5
27.0
27.5
6.0
4.5
3.0
1.5
0.0
−1.5
31.2
32.0
32.8
33.6
34.4
35.2
WGSW
WGIW
LSW
NEADW
TrW$_{Tmax}$
DSOW
AW
TrW
BBMW
BBBW
cold AW
B)
^{236}U (10^6 at/kg)
^{129}I (10^7 at/kg)
0
3
6
9
12
15
18
0
60
120
180
240
300
AR7W Line
central Baffin Bay
Northern Labrador Sea Line
Davis Strait
Northern Line
AW
BBMW
BBBW
cold AW
DSOW
LS Surface
LSW
NEADW
TrW$_{Tmax}$
TrW
WGIW
WGSW

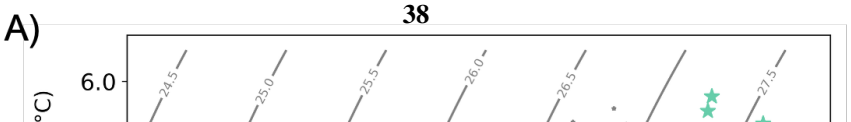
A)
6.0

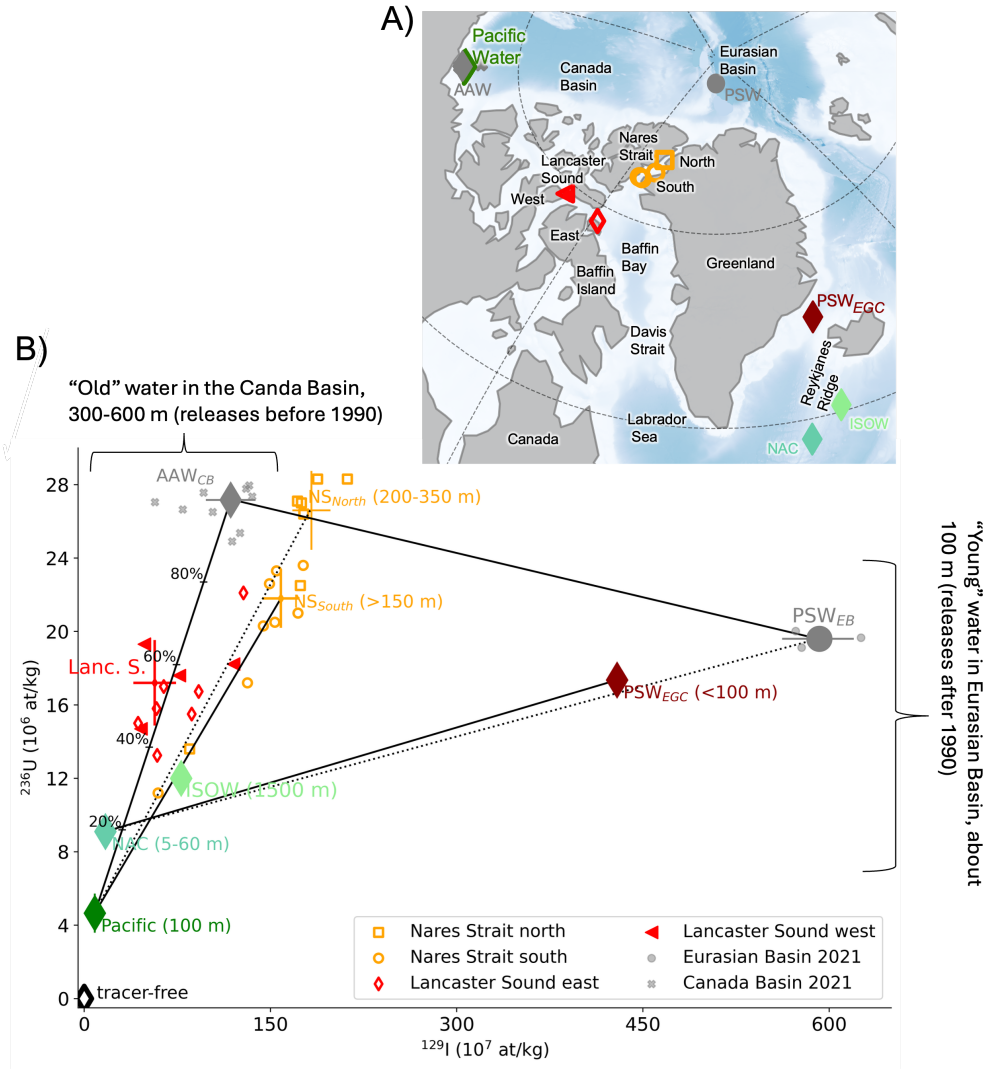

Figure 5. Symbols and colours in panels **A)** ~~Location~~ and **B)** consistently denote water mass endmembers (colored diamonds and circle), previously published Arctic Ocean data (grey diamond and circle), and new data from Lancaster Sound (red symbols) and Nares Strait (orange symbols). **A)** Geographic distribution of ~~each endmember~~ endmembers and ~~the samples~~ sampling locations in the Arctic Ocean, ~~used to derive the endmembers~~Nares Strait, and Lancaster Sound. **B)** ^{129}I~~–~~–^{236}U tracer space ~~with~~ showing endmembers ~~indicated by diamonds~~ and individual samples ~~reported in this study shown with light grey crosses~~at Nares Strait and Lancaster Sound. ~~Published data from the Arctic Ocean is indicated by~~ Red crosses indicate the mean and ~~circles. Data~~ maximum spread of measurements from the upper 100 m in western Lancaster Sound~~(red symbols)~~ , while the orange cross represents the mean and maximum spread of samples from southern Nares Strait ~~(orange symbols) have not been published before~~collected below 150 m. Numbers adjacent to the endmembers denote the depth ranges of the samples used in their calculation. AAW~~$_{CB}$~~$_{CB}$: Arctic Atlantic Water in Canada Basin (Payne et al., 2024)~~,~~. NAC: North Atlantic current (Castrillejo et al., 2018)~~, PSW-EGC~~. PSW$_{EGC}$: Polar Surface Water at the East Greenland Current (Dale et al., 2024)~~,~~. Pacific Water (Payne et al., 2024)~~,~~. PSW~~central Arctic~~$_{EB}$: Polar Surface Water in the ~~central Arctic~~ Eurasian Basin (Wefing et al., 2025). Tracer-free: very old ~~waters~~ water without anthropogenic signature, glacier and sea ice melt, river runoff, and precipitation.

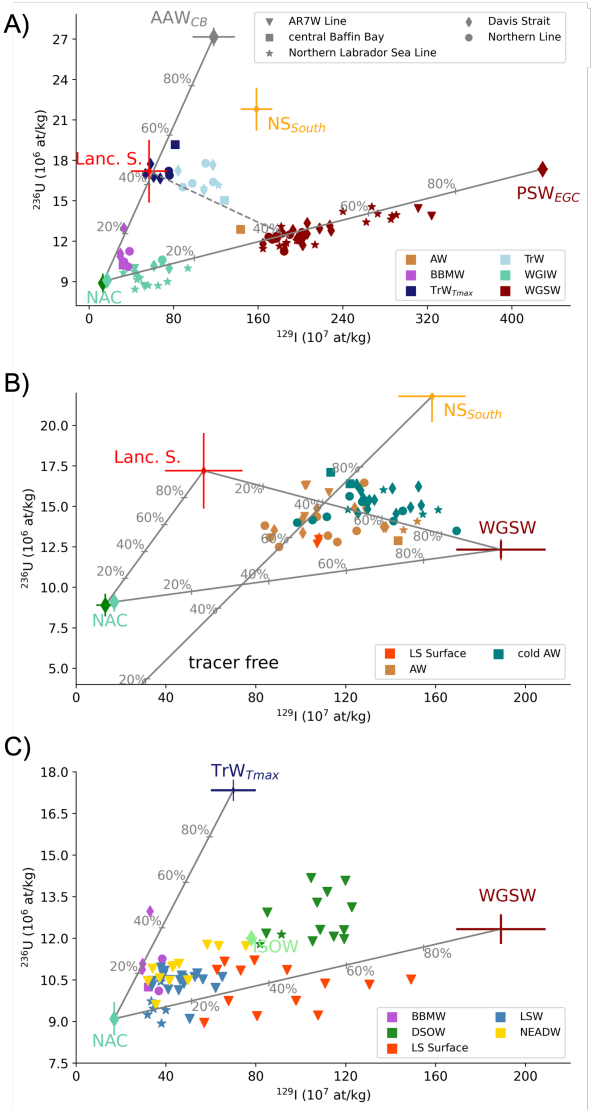

Figure 6. Binary mixing model of ^{129}I ~~versus~~ vs. ^{236}U used to infer water mass origins and mixing. Symbol ~~shape indicates~~ shapes indicate sampling locations: central Baffin Bay (~~square~~squares), Northern Line (dots), ~~Mooring Line~~ Davis Strait (diamonds), Northern Labrador Sea Line (stars), and AR7W (triangles). Colored diamonds mark endmembers, with crosses showing endmembers defined in this study, including their maximum spread. The ~~solid~~ line ~~represents mixing between~~ connecting the endmembers ~~; dashed~~ represent mixing lines~~show each endmember's contribution to a sample~~, ~~and dotted~~ while number along the mixing lines ~~interpolate samples to~~ denotes the mixing ~~line. Capital letters label distances for mixing~~ fraction~~calculations (see Section 4), while lowercase letters (a–h) highlight samples discussed further~~. ~~Panels show binary mixing models for:~~ The water masses presented in the panels are selected based on their tracer properties. **A)** ~~Transition Water (TrW),~~ Maximum tracer concentrations in the study region are represented by West Greenland Shelf Water (WGSW), West Greenland Irminger Water (WGIW), and Baffin Bay Mode Water (BBMW)~~;~~. Additionally, Transition Water (TrW) is also represented with special emphasis on its temperature maximum (TrW$_{Tmax}$ dark blue symbols). **B)** ~~cold~~ Mixing between Arctic Water (~~cold~~ AW) ~~,~~ and cold Arctic Water (cold AW) ~~, and Transition Water mix;~~ in Baffin Bay. **C)** Mixing in the Labrador Sea, including: Labrador Sea Water (LSW), Labrador Sea Surface ~~water~~Water, and North East Atlantic Deep Water (NEADW). References, sample counts, and sampling years for endmembers are listed in Appendix Table A2. ~~Acronyms~~ Abbreviations are explained in Appendix ~~A~~ Table A1.

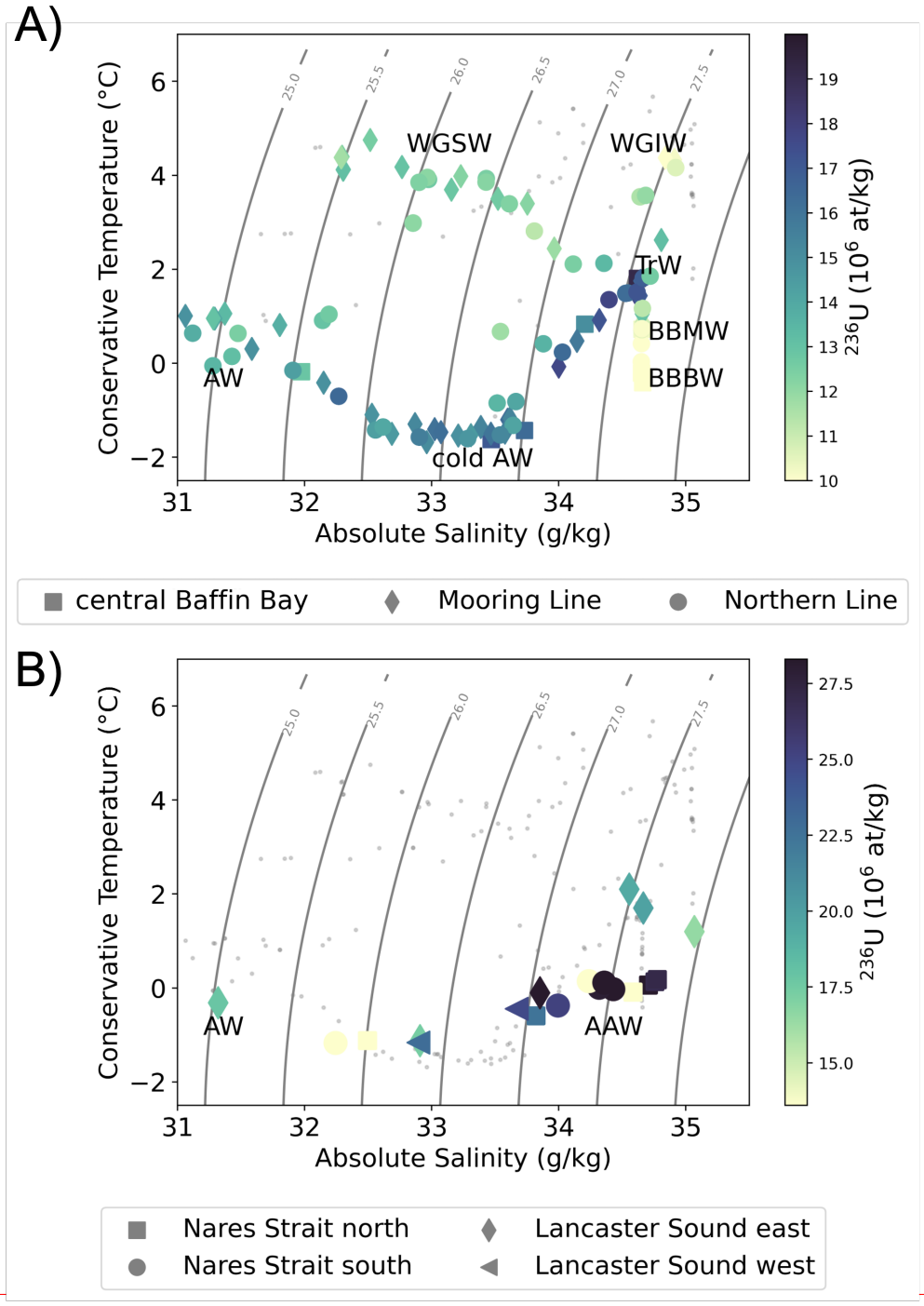
A)
Conservative Temperature (°C)
Absolute Salinity (g/kg)
25.0
25.5
26.0
26.5
27.0
27.5
WGSW
WGIW
TrW
BBMW
BBBW
AW
cold AW
^{236}U (10^6 at/kg)
central Baffin Bay
Mooring Line
Northern Line
B)
Conservative Temperature (°C)
Absolute Salinity (g/kg)
AW
AAW
^{236}U (10^6 at/kg)
Nares Strait north
Nares Strait south
Lancaster Sound east
Lancaster Sound west

A1 Appendix A, ~~Acronyms~~Abbreviations

Table A1. Appendix A: ~~Acronyms, Water Masses, and Currents: The~~ Abbreviations of water masses ~~referenced~~ and currents cited in ~~this study~~ the manuscript. Water mass definitions are based on classifications from Curry et al. (2014), Huang et al. (2024), García-Ibáñez et al. (2015), Yashayaev (2007) and Bourke et al. (1989). In this work, hydrographic properties are reported as follows: Absolute ~~Salinity~~ salinity (S_A, g/kg) and ~~Conservative Temperature~~ conservative temperature (CT, °C) are given for all data newly analysed in this study, following TEOS-10 recommendations. For water masses described in the literature whose properties were not re-evaluated here, values are reported as practical salinity ~~(PSU)~~ and potential temperature (T_{pot}, °C), following the original sources. This approach ensures consistency with both current standards (TEOS-10) and historical literature for all water mass and current definitions~~presented~~.

Acronym	Water mass / current	Salinity	Temperature	Refe
AAW~~$_{CB}$~~ CB	Arctic Atlantic Water Canada Basin	>34.7	T_{pot}>0	Payne et
AAW$_{CAA}$	Arctic Atlantic Water	S_A> 33	CT ~~>~~< -1	this
AW	Arctic Water	S_A> 32.9	~~1.1 >CT>~~ CT: -0.8 – 1.1	this
AW$_{CAA}$	Arctic Water CAA	S_A < 33	CT < 0	this
BBBW	Baffin Bay Bottom Water	S_A: 34.6	CT< 0.4	this
BBMW	Baffin Bay Mode Water	S_A: 34.6	CT: 0.7 ~~–~~– 1.2	this
cold AW	cold Arctic Water	~~32.5 <~~S_A~~<~~: 32.5 – 33.8	CT< -0.8	this
DSOW	Denmark Strait Overflow Water	S_A< 35 ±0.1	CT< 1.3	this
ISOW	Iceland–Scotland Overflow Water	34.9-35 PSU	T_{pot}: 2.0 ~~-3.5~~ – 3.5	Dale et a
LSW	Labrador Sea Water	S_A> 35	~~3.0 -~~ CT: 3.1 – 3.8	this
NEADW	North East Atlantic Deep Water	~~35.06~~35.07±0.2	~~2.4 -~~ CT: 2.0 – 3.3	this
Pacific Water	Pacific Water	<32.5 PSU	T_{pot}-0.4±0.1	Payne et
PSW~~central Arctic~~ EB	Polar Surface Water Eurasian Basin	density: σ_θ <27.70		Wefing et
~~PSW-EGC~~ PSW$_{EGC}$	Polar Surface Water at Denmark Strait	<34.3 PSU	T_{pot}< 0	Dale et a
SAIW	Subarctic Intermedaite Water	34.9 PSU	T_{pot}: ~~4-7~~ 4 – 7	Castrillejo
TrW	Transition Water	S_A: 34.0 – 34.6 ~~±0.2~~	~~1.4 -~~ CT: 0 – 1.8	this
TrW~~mix~~ T_{max}	~~Transition Water mix~~ Temperature maximum in TrW	S_A: ~~34-34.5~~ 34.64±0.03	CT~~<~~: 1.4 – 1.8	this
WGIW	West Greenland Irminger Water	S_A >34.7	CT> 3.5	this
WGSW	West Greenland Shelf Water	S_A< 34.2	CT< 5	this

BIC	Baffin Island Current
CAA	Canadian Arctic Archipelago
EB	Eurasian Basin
EGC	East Greenland Current
Lanc. S.	Lancaster Sound
LC	Labrador Current
LS	Labrador Sea
NAC	North Atlantic Current
NCC	Norwegian ~~Coastel~~ Coastal Current
NS$_{South}$	southern Nares Strait
WGC	West Greenland Current

Table A2. Endmember ~~Data~~ data with ~~Geographic~~geographic location and depth, ~~Isotopic,~~ concentrations of ^{129}I and ~~Hydrographic Properties~~^{236}U and hydrographic properties.

Endmember	Latitude °N	Longitude °E	Depth (m)	^{129}I ($\times 10^7$ at/kg)	^{236}U ($\times$1
AAW~~$_{CB}$ CB~~ $_{CB}$	70.6 ~~–~~ – 77.7	-140.0 ~~–~~ – -146.8	300 – 600	118 ± 20	27.2 ±
~~Pacific~~ ISOW	~~70.6 – 77.7~~ 55.3	~~-140.0 – -146.8~~ -26.4	~~8.5~~ 1500	78 ± ~~2.4~~ 2	~~4.6~~ 12.0 ±
~~PSW-EGC~~ Lanc. S.	~~67.5~~ 74.1	~~-25.8~~ -91.1	~~429~~ < 100	57±~~5~~ 17	~~17.3~~ 17.2 ±
NAC	58.5	-31.2	~~16.93~~ 5 – 60	16.9 ± 0.4	9.1 ±
~~ISOW~~ NS$_{South}$	~~55.3 -26.4 78 ± 2 12 ± 0.1 35.14 ± 0.01 2.7 ± 0.1 3 b NSSouth~~ 78.3	-73.3 ~~–~~ - ~~–~~ –74.7	> 150	158 ± 15	21.8 ±
Pacific	70.6 – 77.7	-140.0 – -146.8	100	8.5 ± 2.4	4.6 ±
PSW$_{EGC}$	67.5	-25.8	< 100	429 ± 5	17.3 ±
WGSW	63.7 ~~–~~ – 69.2	-53.0 ~~–~~ – -58.4	400 – 650	189 ± 20	12.3 ±
TrW	66.7 ~~–~~ – 72.7	-57.3 ~~–~~ – -65.9	5 – 300	70 ± 10	17 ±

~~*PSW-EGC corresponds to PSW at Denmark Strait, a:Payne et al. (2024), b:Dale et al. (2024), c:Castrillejo et al. (2018), d: this study*~~a: Payne et al. (2024), b: Dale et al. (2024), c: Castrillejo et al. (2018), d: this study.

Water mass and location	**Fraction f**	**Mixing line $\overrightarrow{b}$**
NS_{South}	up to 25% NS_{North}	NS_{North} – Pacific
Lancaster Sound	55-65% AAW_{CB}	AAW_{CB} – Pacific
$WGSW_{ARTW}$	up to 70% PSW_{EGC}	PSW_{EGC} – NAC
$WGSW_{Davis\ Strait}$	40% PSW_{EGC}	PSW_{EGC} – NAC
$WGIW_{Davis\ Strait}$	15% PSW_{EGC}	PSW_{EGC} – NAC
$AW_{central\ Baffin\ Bay}$	75% WGSW	WGSW – NAC
AW_{BIC}	55% WGSW	Lanc. S. – WGSW
$AW_{Labrador\ Current}$	70% NS_{South}	NS_{South} – Pacific
cold $AW_{central\ Baffin\ Bay}$	70% NS_{South}	NS_{South} – Pacific
cold $AW_{Northern\ Line}$	80% WGSW	WGSW – NAC
TrW_{Tmax}	60-65% AAW_{CB}	AAW_{CB} – Pacific
LSW	up to 30% WGSW	WGSW – NAC
LSW	up to 20% TrW_{Tmax}	TrW_{Tmax} – WGIW
LS Surface	up to 70% WGSW	WGSW – NAC
NEADW	up to 25% TrW_{Tmax}	TrW_{Tmax} – WGIW

A2 Appendix B, Additional Figures

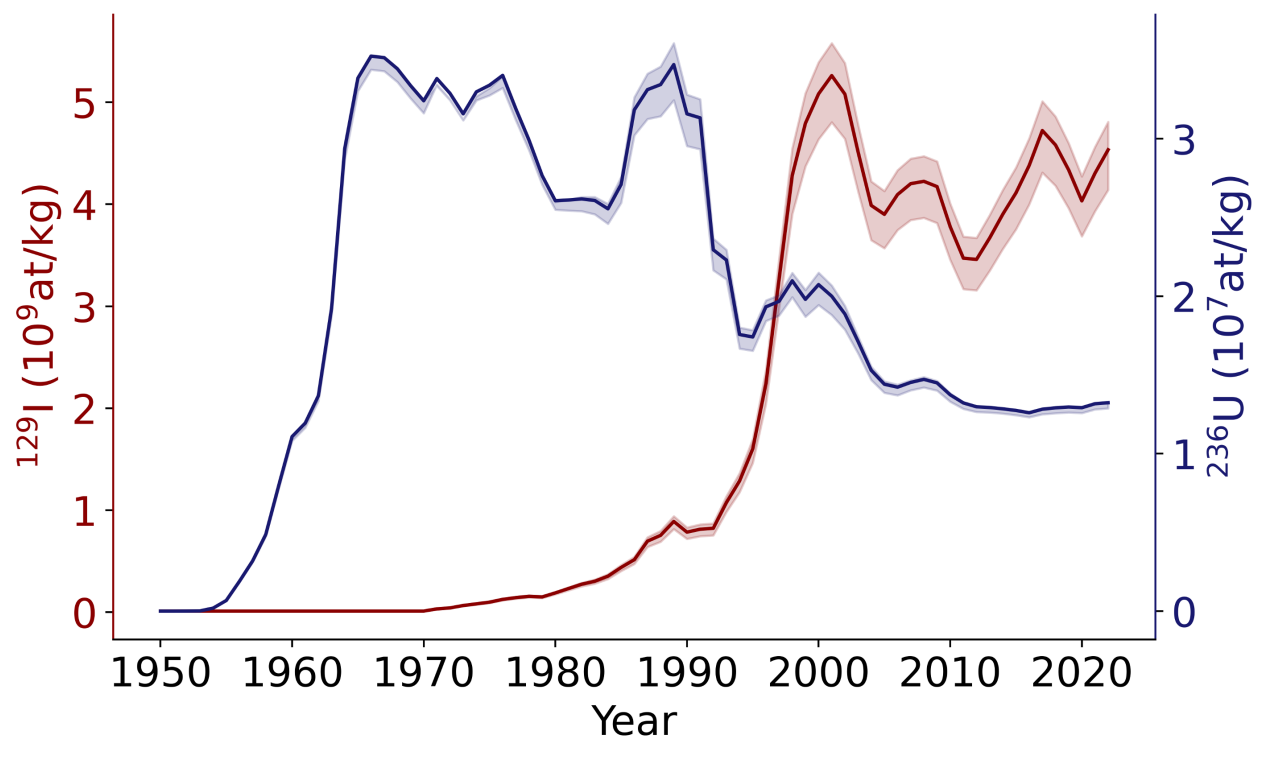

Figure A1. Input function of ^{129}I (red) and ^{236}U (blue) defined at 70°N in northern Norway showing the combined ~~imput~~ input from nuclear fuel reprocessing plants in Sellafield (UK) and La Hague (F), and the global fallout from atmospheric nuclear weapon tests (Wefing et al., 2021; Payne et al., 2024).

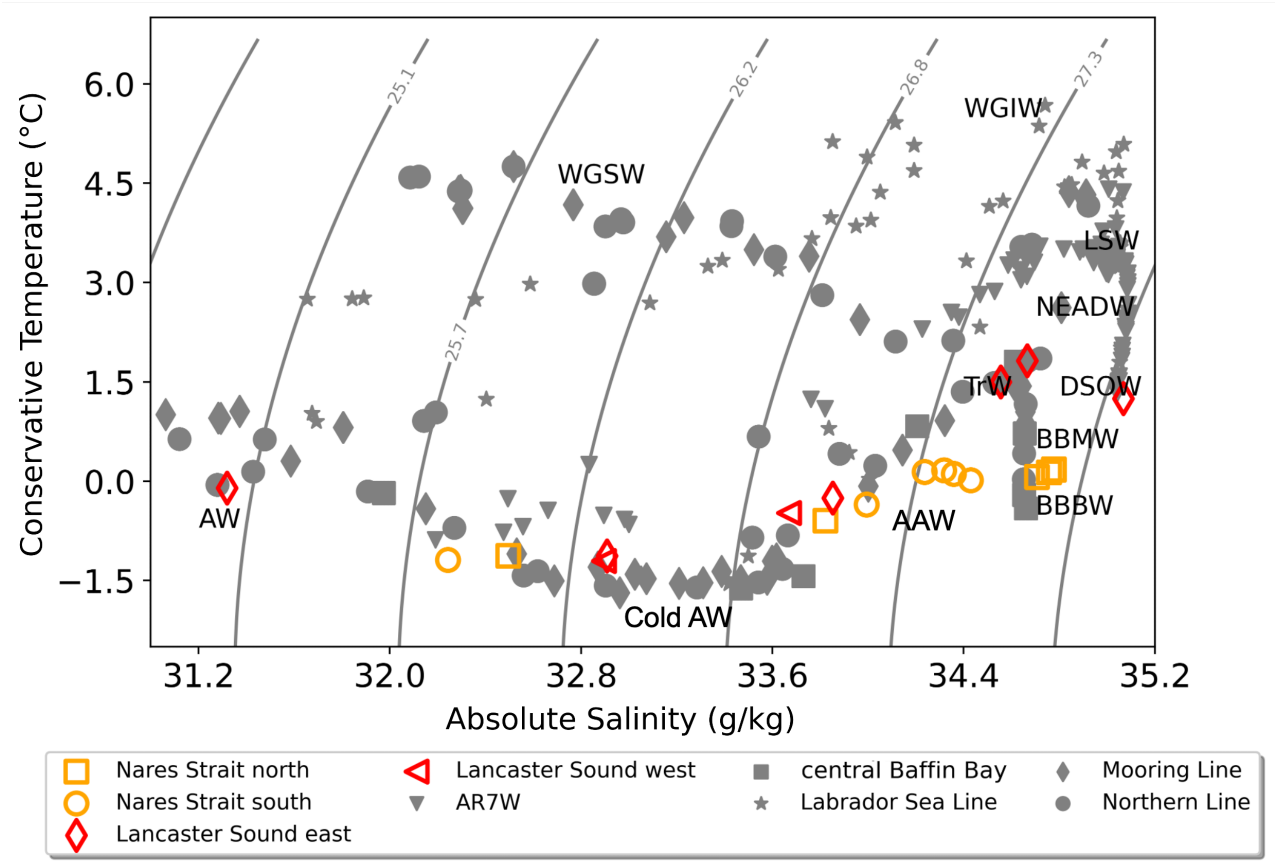

Figure A2. T — S diagram of all samples reported in this study. Grey symbols represent the samples covering the four lines and central Baffin Bay sampled in 2022. The red symbols represent samples from Lancaster Sound, while the orange symbols represent the samples from Nares Strait, both sampled in 2024.

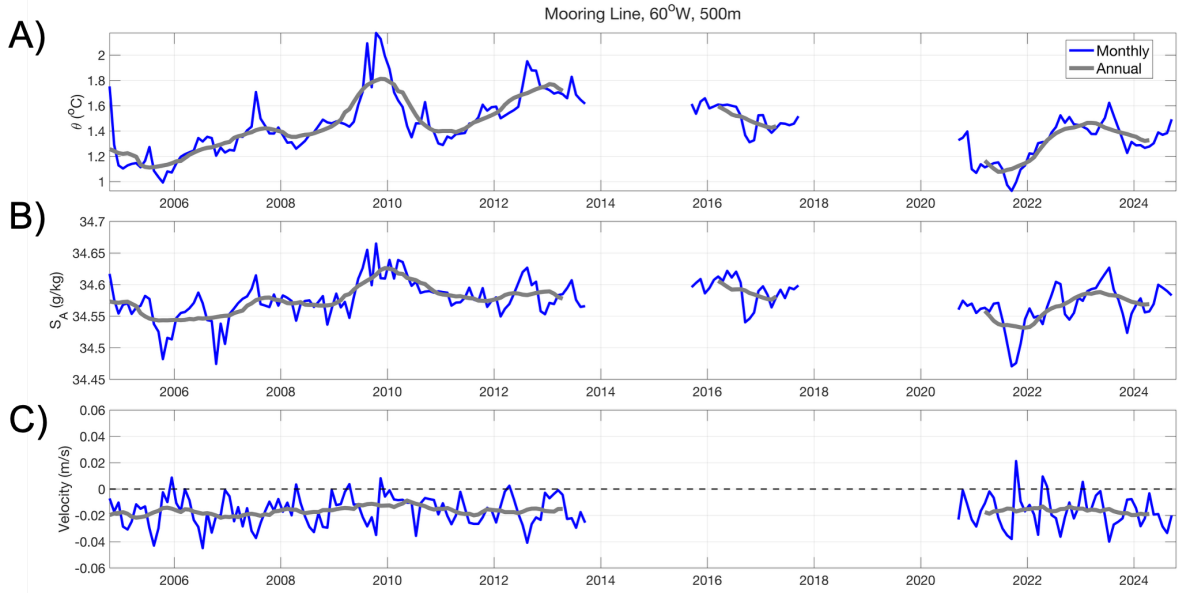
Mooring Line, 60°W, 500m
A)
B)
C)
Monthly
Annual
θ (°C)
S_A (g/kg)
Velocity (m/s)
2006
2008
2010
2012
2014
2016
2018
2020
2022
2024

1135

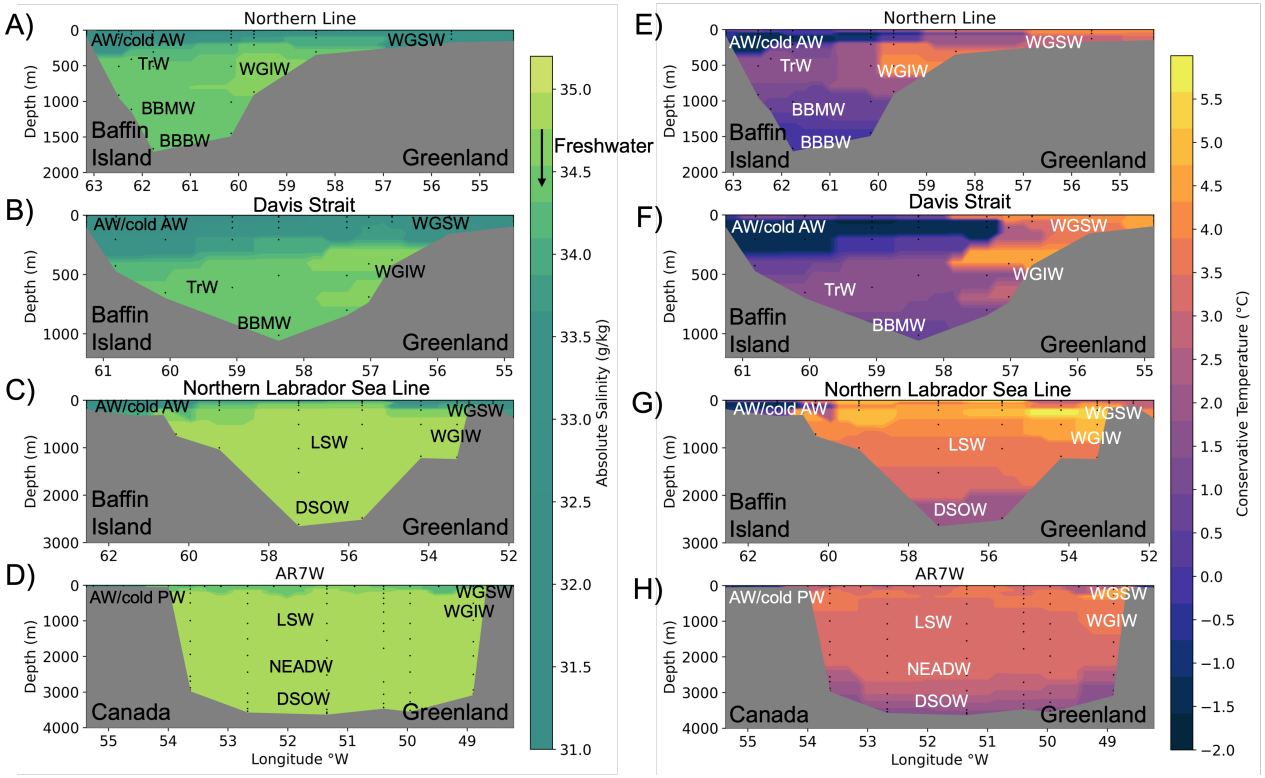

Figure A3. Section plots of ~~Absolute Salinity~~ absolute salinity (~~A–D~~A – D) and ~~Conservative Temperature~~ conservative temperature (~~E–H~~E – H), along the Northern Line (A, E), ~~Mooring Line~~ Davis Strait (~~B–F~~B, F), Northern Labrador Sea Line (C, G), and AR7W Line (D, H).